THE JOURNAL OF BIOLOGICAL CHEMISTRY
Vol. 279, No. 38, Issue of September 17, pp. 39454-39464, 2004
Printed in U.S.A.

Interleukin (IL)-4-independent Maintenance of Histone Modification of the IL-4 Gene Loci in Memory Th2 Cells*[S]

Received for publication, May 28, 2004, and in revised form, July 14, 2004
Published, JBC Papers in Press, July 16, 2004, DOI 10.1074/jbc.M405989200

Masakatsu Yamashita, Ryo Shinnakasu, Yukiko Nigo, Motoko Kimura, Akihiro Hasegawa, Masaru Taniguchi‡, and Toshinori Nakayama§

From the Department of Immunology, Graduate School of Medicine, Chiba University, 1-8-1 Inohana Chuo-ku, Chiba 260-8670 and the ‡Laboratory for Immune Regulation, RIKEN Research Center for Allergy and Immunology, Yokohama, 230-0045, Japan

Interleukin (IL)-4-induced STAT6 activation and the subsequent up-regulation of GATA3 are crucial for the induction of chromatin remodeling of the Th2 cytokine gene loci as Th2 cells undergo development. This study probes the role of these molecules in the maintenance of memory Th2 cells. IL-4 was not required to maintain the capability for Th2 cytokine production in *in vivo* generated antigen-specific memory Th2 cells. Histone H3-K9/14 hyperacetylation and intergenic transcripts associated with the *IL-4* gene locus were preserved in the absence of IL-4, but those associated with the *IL-13* gene were partially IL-4-dependent. Histone H3-K4 methylation of the *IL-13* and *IL-4* gene loci was fully preserved in memory Th2 cells and accompanied by memory cell-specific accumulation of Pol II complex to highly restricted sites. Thus, memory Th2 cells maintain a unique Th2-specific remodeled chromatin in the *IL-4* and *IL-13* gene loci by active molecular events that are IL-4-independent.

After TCR[1] recognition of antigens, naïve CD4 T cells differentiate into two distinct helper T (Th) cell subsets, Th1 and Th2 cells (1). Th1 cells produce IFNγ, and direct cell-mediated immunity against intracellular pathogens. Th2 cells produce IL-4, IL-5, and IL-13, and are involved in humoral immunity and allergic reactions. The direction of Th cell differentiation depends on the cytokine environment (2, 3). Naïve CD4 T cells stimulated with antigens in the presence of IL-12 differentiate into Th1 cells, whereas IL-4 drives differentiation into Th2 cells (4–6). The IL-12-mediated activation of signal transducer and activator of transcription (STAT) 4 is crucial for Th1 cell differentiation, while IL-4-mediated STAT6 activation is for Th2 cell development (7–9). In addition to the cytokines mentioned above, TCR stimulation by antigens also influences the direction of Th1/Th2 cell differentiation. We reported that efficient TCR-mediated activation of the $p56^{lck}$, calcineurin, and Ras-ERK MAPK signaling cascade was required for Th2 cell differentiation (10–12).

Recently, several transcription factors that control Th2 cell differentiation were identified (13, 14). Among them, GATA3 appears to be a master transcription factor for Th2 cell differentiation. GATA3 is selectively expressed in Th2 cells, and its ectopic expression induces Th2 cell differentiation even in the absence of STAT6 (15–18).

Changes in the chromatin structure of the Th2 cytokine (*IL-4/IL-5/IL-13*) gene loci occur during Th2 cell differentiation (19, 20). Recent studies have demonstrated that covalent modifications of histones play critical roles in epigenetic regulation (21). Recently, we and others (22–24) demonstrated that histone hyperacetylation of the Th2 cytokine gene loci occurs in developing Th2 cells in a Th2-specific and STAT6-dependent manner. Also, we demonstrated an essential role for GATA3 in Th2-specific histone hyperacetylation (22). We generated a precise map of the Th2-specific histone hyperacetylation within the type 2 cytokine gene loci, and identified a 71-bp conserved GATA3 response element (CGRE) at 1.6-kbp upstream of the *IL-13* locus exon 1. The CGRE appears to play a crucial role for GATA3-mediated targeting and downstream spreading of core histone hyperacetylation within the *IL-13* and *IL-4* gene loci in developing Th2 cells and Tc2 cells (22, 25).

Histone lysine methylation is considered to be a key epigenetic regulator (26). Methylation of specific lysine residues of histones is required for the maintenance of large, functionally distinct chromatin domains, such as heterochromatin correlated with histone H3 lysine 9 (H3-K9) (27). In contrast, transcriptionally active euchromatin preferentially contains methylated histones at H3-K36, H3-K79, and H3-K4 sites (28). Particularly, methylation at H3-K4 correlates well with active or permissive state of transcription (29). Furthermore, yeast Set1 (H3-K4 methyl-transferase) and Set2 (H3-K36 methyl-transferase) induce histone lysine methylation and functionally interact with RNA polymerase II (Pol II), suggesting that histone methylation at H3-K4 and H3-K36 is a hallmark of actively transcribed chromatin (26).

Some of the differentiated Th2 cells survive and are main-

* This work was supported by grants from the Ministry of Education, Culture, Sports, Science, and Technology (Japan) (Grants-in-aid of Scientific Research, Priority Areas Research 13218016; Scientific Research B 14370107, Advanced and Innovational Research program in Life Science and Special Coordination Funds), the Ministry of Health, Labor and Welfare (Japan) (a grant-in-aid for Research on Advanced Medical Technology), the Program for Promotion of Fundamental Studies in Health Science of the Organization for Pharmaceutical Safety and Research (Japan), the Human Frontier Science Program Research Grant (RG00168/2000-M206), and the Hamaguchi Foundation and Uehara Memorial Foundation. The costs of publication of this article were defrayed in part by the payment of page charges. This article must therefore be hereby marked "*advertisement*" in accordance with 18 U.S.C. Section 1734 solely to indicate this fact.

[S] The on-line version of this article (available at http://www.jbc.org) contains Supplementary Data.

§ To whom correspondence should be addressed: Dept. of Immunology, Graduate School of Medicine, Chiba University, 1-8-1 Inohana, Chuo-ku, Chiba 260 Japan. Tel.: 81-43-226-2200; Fax: 81-43-227-1498; E-mail: tnakayama@faculty.chiba-u.jp.

[1] The abbreviations used are: TCR, T cell antigen receptor; Th2, type-2 helper T; CGRE, conserved GATA3 response element; STAT, signal transducer and activator of transcription; CAR, Coxsackie/adenovirus receptor; EGFP, enhanced green fluorescence protein; HAT, histone acetyl transferase; ChIP, chromatin immunoprecipitation; STAT6-KO, STAT6-deficient; IL, interleukin; FITC, fluorescein isothiocyanate; Pol II, polymerase II; mAb, monoclonal antibody; WT, wild type; ELISA, enzyme-linked immunosorbent assay; IFN, interferon.

tained as memory Th2 cells for a long period *in vivo* (30, 31). Memory CD4 T cells can be generated from effector cells and can survive in the absence of MHC antigens (32, 33). The expression of either TCR (34) or Src-family kinases, $p56^{lck}$ and $p59^{fyn}$ appears not to be essential for the long-term survival (35). Also CD4 T cell survival is not directly linked to MHC-induced TCR signaling (36). In class II-restricted TCR transgenic mice lacking expression of the common cytokine receptor γ-chain (γc), the survival of naïve T cells is substantially impaired but memory T cell survival is apparently normal, suggesting that γc-dependent cytokines (IL-2, IL-4, IL-7, IL-9, and IL-15) is not required for memory CD4 T cell survival (37). As for homeostatic proliferation of CD4 memory T cells, IL-7 and IL-15 are not essential (33). Thus, in contrast to CD8 memory T cells, CD4 memory cells may not require any specific cytokine signals for their homeostatic maintenance (38, 39). Very recently, however, regulatory roles of IL-7 in the generation and survival of memory CD4 T cells were reported (40, 41). In addition, signals through the TCR as well as the IL-7 receptor appear to regulate the homeostasis of CD4 memory T cells (42). Th1 memory cells appear to be generated efficiently from an IFNγ non-producing population (43). Thus, it is still unclear whether any specific signals including those triggered by cytokines are required for the maintenance of memory Th2 cells. Furthermore, the molecular mechanisms that underlie the maintenance of capacity for Th2 cytokine production in memory Th2 cells, particularly those that preserve the Th2-specific remodeled chromatin are not fully understood.

In the present study, we used an adoptive transfer technique for the generation of antigen-specific memory Th2 cells *in vivo* to investigate the molecular events governing the maintenance of their Th2-specific cytokine production. In freshly prepared *in vivo* generated memory Th2 cells, histones associated with the *IL-4* and *IL-13* gene loci were hyperacetylated (at H3-K9/14) and di- and tri-methylated (at H3-K4), and these events were seen IL-4-deficient situation as well. Intergenic transcripts accompanied by highly localized accumulation of Pol II to CNS1, *IL-4* promoter, and V_A enhancer sites were observed. Thus, Th2-specific remodeled chromatin of the *IL-13* and *IL-4* gene loci is maintained in memory Th2 cells by active molecular events that are IL-4-independent.

EXPERIMENTAL PROCEDURES

Mice—BALB/c and BALB/c *nu/nu* mice were purchased from Clea Inc., Tokyo, Japan. IL4-deficient mice (44) and OVA-specific TCRαβ transgenic (DO.11.10 Tg) mice (45) were maintained under SPF conditions. All mice used in this study were maintained under specific pathogen-free conditions. Animal care was in accordance with the guidelines of Chiba University.

Reagents—The reagents used in this study are as follows: Fluorescein isothiocyanate (FITC)-conjugated anti-CD4 mAb (GK1.5-FITC), anti-CD62L mAb (MEL-14), anti-CD25 mAb (7D4), anti-CD69 mAb (H1.2F3), phycoerythrin (PE)-conjugated anti-CD4 mAb (GK1.5-PE), anti-CD44 mAb (IM7-PE), anti-CD122 mAb (TM-b1), anti-CD124 mAb (mIL-4R-M1), anti-CD127 mAb (4G3), and anti-CD132 mAb (TUGm2) were purchased from BD PharMingen, San Diego, CA. Anti-FcRgII and III mAb (2.4G2) and unconjugated anti-IL-4 mAb (11B11) were used as culture supernatants. Recombinant mouse IL-12 was purchased from BD PharMingen and recombinant mouse IL-4 was from TOYOBO, Osaka, Japan. The OVA peptide (residues 323–339; ISQAVHAAHAEINEAGR) was synthesized by BEX Corporation, Tokyo, Japan.

The Generation of Effector and Memory Th1/Th2 Cells—Splenic CD4 T cells from DO11.10 OVA-specific TCR transgenic (Tg) mice were stimulated with an OVA peptide (Loh15, 1 μg/ml) plus APC under Th1- or Th2-skewed conditions for 5 days *in vitro* (10). We used these cells as effector Th1 or Th2 cells, respectively. The effector Th1/Th2 cells (3×10^7) were transferred intravenously into normal syngeneic BALB/c or BALB/c *nu/nu* recipient mice. In most of the experiments, 4 weeks after the cell transfer, KJ1$^+$ cells in the spleen were sorted by FACSVantage™ (BD PharMingen), and used as memory Th1and Th2 cells.

Cell Cycle Analysis—Splenic KJ1$^+$ cells were isolated by auto-MACS (Militenyi Biotec) with yielding purity >95%. The cells were fixed with 70% ethanol for 12 h, treated with RNase for 10 min at 37 °C and then suspended in 50 μg/ml PI (propidium iodide) solution. DNA contents were analyzed by flow cytometry.

Detection of Cell Division—Memory Th2 cells were prepared by sorting 4 weeks after cell transfer, and were labeled with CFSE (carboxyfluorescein diacetate succinimidyl ester, Molecular Probes) as described previously (46). Labeled cells were stimulated with OVA peptide (0.1 or 1 μM) plus APC for 16 h, and then subjected to flow cytometry.

ELISA—Cytokine production was assessed by ELISA as described (25).

Chromatin Immunoprecipitation (ChIP) Assay—Acetylation status of histone H3-K9/K4 was assessed using histone H3 (K9/14) ChIP assay kits (17-245; Upstate Biotechnology) and specific primers described in supplemental data. The ChIP assay for di- or tri-methylated histone H3-K4 was performed using anti-histone H3 di-methyl K4 antiserum (07–030; Upstate Biotechnology) and anti-histone H3 trimethyl K4 antiserum (ab7766; Abcam). The ChIP assay for GATA3, Pol II, and TFIIB was done as described (22). An anti-RNA polymerase II antiserum (C-21) and anti-TIFIIB (C-18) anti-serum was purchased from Santa Cruz Biotechnology (Santa Cruz, CA).

RT-PCR—RT-PCR analyses for GATA3, GATA3a, GATA3b, cytokines, β-actin, and intergenic regions of IL-13 and IL-4 were done as described (25).

Immunoblot Analysis—Immunoblot analyses for GATA3 and tubulin-α were done as described (25).

RESULTS

Generation of Antigen-specific Memory Th2 Cells in Vivo—We first established an experimental system where antigen-specific memory Th2 cells are generated and maintained efficiently *in vivo*. Splenic CD4 T cells from DO11.10 OVA-specific TCR transgenic (Tg) mice were stimulated with an OVA peptide (Loh15) plus APC under Th2-skewed conditions for 5 days *in vitro*, and then transferred intravenously into normal syngeneic BALB/c or BALB/c *nu/nu* recipient mice. The transferred DO11.10 Tg T cells were monitored by staining with the clonotypic KJ1 mAb. Typical staining patterns and the percentages of KJ1$^+$ cells/CD4$^+$ cells in BALB/c recipient mice are shown in Fig. 1*A*. A week after transfer, ~25% of splenic CD4 T cells were KJ1-positive. The numbers of KJ1$^+$ cells decreased at ~10% at the 2 week time point, and this level was maintained for at least for 16 weeks. Similar kinetics was observed in BALB/c *nu/nu* recipient mice (data not shown). A typical KJ1/CD4 staining pattern of spleen cells of BALB/c *nu/nu* recipient mice at 4 weeks after cell transfer, and DNA contents of the recovered KJ1$^+$ CD4$^+$ cells are shown in Fig. 1*B*. The PI staining profiles of the recovered KJ1$^+$ CD4$^+$ cells were indistinguishable from those of freshly isolated KJ1$^+$ cells from DO11.10 Tg mice, and almost all KJ1$^+$ cells were in G_0/G_1 phase.

Memory T cells proliferate rapidly in response to a low concentration of antigens as compared with naïve T cells (47). *In vivo* generated KJ1$^+$ memory Th2 cells in BALB/c *nu/nu* mice at the 4 week time point were purified by cell sorting (<98%), labeled with CFSE, and stimulated with two different doses of OVA peptides and APC for 16 h. Cell division analysis by flow cytometry showed that freshly isolated CD4 T cells from DO11.10 Tg mice did not proliferate during the first 16 h after stimulation, whereas substantial numbers of memory Th2 cells divided once in response to the antigenic peptide (27.4% for 0.1 μM and 37.9% for 1 μM OVA peptides) (Fig. 1*C*).

Next we assessed the expression levels of cell surface molecules including activation and memory markers and cytokine receptors on the freshly isolated memory Th2 cells (Fig. 1*D*). The expression levels of IL-4 receptor (R)α and common γ (cγ) chains were slightly higher in memory Th2 cells compared with those of freshly isolated KJ1$^+$ cells from DO11.10 Tg mice. Dramatically increased levels of IL-2Rβ and IL-7Rα chains were observed in memory Th2 cells. The activation markers, CD69 and CD25 (IL-2Rα chain), were not significantly ex-

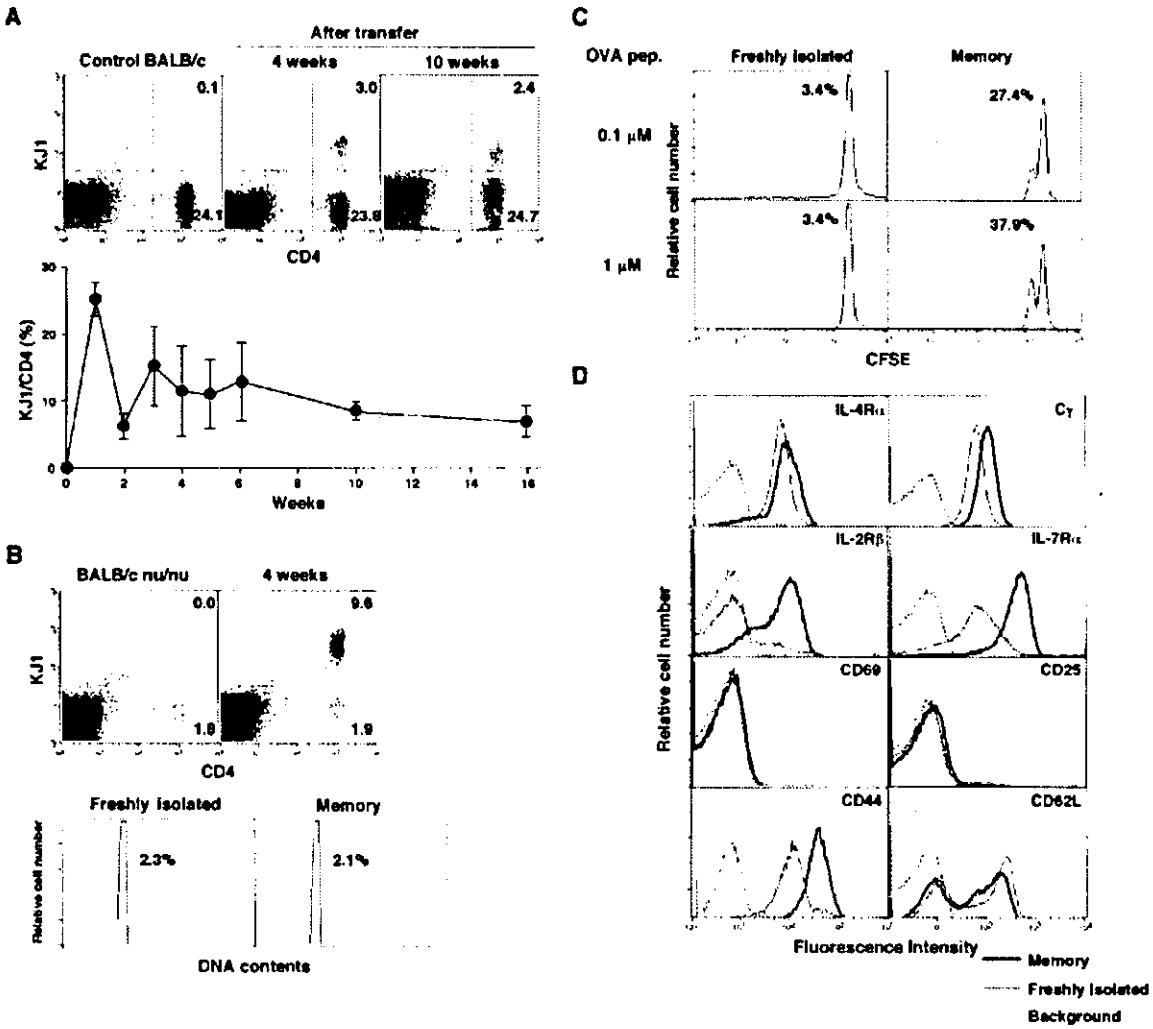

FIG. 1. **Generation and phenotypic characterization of OVA-specific memory Th2 cells.** *A*, kinetics of memory Th2 cell generation. Spleen cells were prepared from recipient BALB/c mice at the indicated time, and the number of recovered KJ1-positive cells was determined by the staining with KJ1 mAb. The typical staining patterns and the mean proportion of KJ1-positive cells in CD4 cells from three individual mice are shown. *B*, cell cycle analysis of memory Th2 cells. Effector Th2 cells were transferred into BALB/c *nu/nu* mice. Four weeks after cell transfer, memory Th2 cells were prepared, stained with PI, and analyzed by flow cytometry. Two independent experiments were done with similar results. *C*, memory Th2 cells rapidly proliferated in response to the antigen. Cells were labeled with CFSE and stimulated with OVA peptides (0.1 or 1 μM) plus APC for 16 h. Cell division of CFSE-labeled cells was analyzed by flow cytometry. The percentages of divided cells are shown in each panel. Two independent experiments were done with similar results. *D*, expression profiles of cell surface maker antigens in memory Th2 cells. Spleen cells from BALB/c *nu/nu* recipient mice (*memory*) and DO11.10 Tg mice (*freshly isolated*) were stained with KJ1 mAb and mAbs against indicated cell surface molecules. Staining profiles of electronically gated KJ1-positive cells are shown.

pressed in either memory or naïve populations. High-level expression of CD44 was observed in all recovered KJ1-positive cells. Finally, two subpopulations with high and low expression of CD62L were observed in memory Th2 cells as well as in naïve T cells.

Cytokine Production Profiles of in Vivo Generated Memory Th2 Cells—We examined the cytokine production profiles of *in vivo* generated memory Th2 cells recovered from BALB/c *nu/nu* recipient mice 4 weeks after cell transfer. Freshly isolated splenic KJ1$^+$ CD4 T cells from DO11.10 Tg mice (Fresh), *in vitro* newly generated effector Th2 cells by stimulation with OVA peptides for 5 days *in vitro* (Effector) and *in vivo* generated memory Th2 cells (memory) were re-stimulated with OVA peptide plus APC for 1–3 days. As shown in Fig. 2*A*, *in vivo* generated memory Th2 cells produced large amounts of Th2 cytokines (IL-4, IL-5, and IL-13). The levels were significantly higher than those of effector Th2 cells particularly on day 3. CD62L expression profiles and cytokine production of the recovered KJ1$^+$ cells were similar in both normal BALB/c and BALB/c *nu/nu* recipient mice (see Supplemental Fig. 1).

We also prepared *in vivo* generated Th1 memory cells to confirm the specificity of cytokine production of memory Th1 and Th2 cells. Splenic CD4 T cells from DO11.10 Tg mice were stimulated with OVA peptide plus APC under Th1- or Th2-skewed conditions for 5 days, and transferred into recipient BALB/c *nu/nu* mice. Four weeks after cell transfer, KJ1$^+$ cells were purified and re-stimulated with OVA peptide plus APC. As shown in Fig. 2B, memory Th2 cells produced large amounts

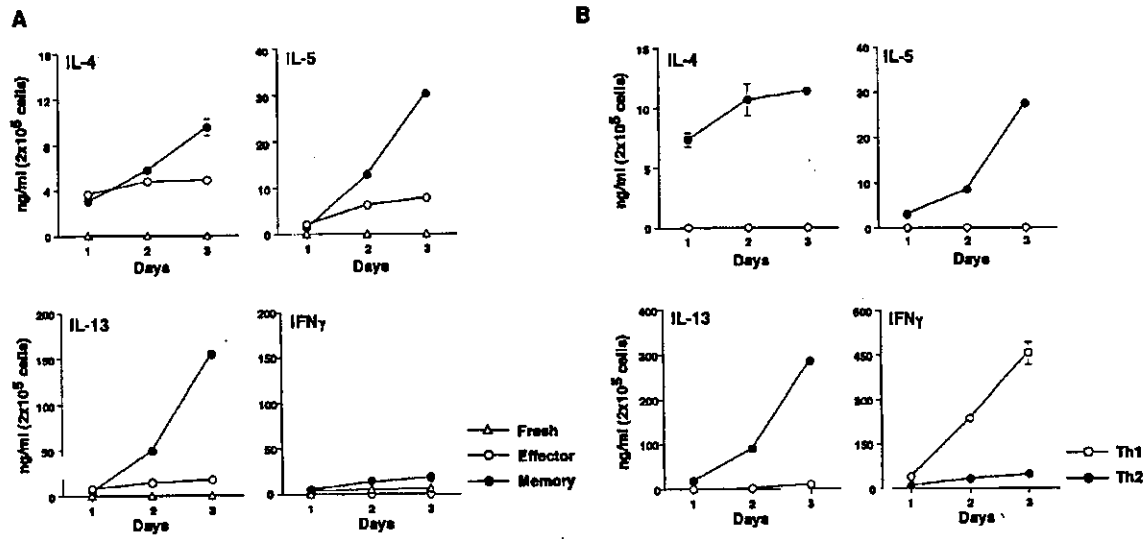

FIG. 2. **Cytokine production profiles of *in vivo* generated memory Th2 cells upon *in vitro* antigenic restimulation.** *A*, freshly isolated splenic KJ1$^+$ CD4 T cells from DO11.10 Tg mice (*Fresh*), *in vitro* newly generated effector Th2 cells by stimulation with OVA peptide for 5 days *in vitro* (*Effector*), and *in vivo* generated memory Th2 cells (*Memory*) were re-stimulated with OVA peptide plus APC for 1, 2, and 3 days. Purified KJ1-positive cells (2×10^6) were restimulated *in vitro* with 1 μM OVA peptide plus APC, and culture supernatants were collected at indicated times. The amounts of the indicated cytokines in the culture supernatant were assessed by ELISA. Four independent experiments with different T cell preparations were done with similar results. *B*, cytokine production profiles of *in vivo* generated memory Th1 and Th2 cells. CD4 T cells from DO11.10 Tg mice were stimulated with OVA peptide (1 μM) plus APC under the Th2-skewed condition or the Th1-skewed condition for 5 days. Then, the effector Th2 and Th1 cells (3×10^7) were transferred into BALB/c *nu/nu* mice intravenously. Four weeks after cell transfer, memory Th2 and Th1 cells were prepared and stimulated with OVA peptide antigens as in *A*. Two independent experiments with different T cell preparations were done with similar results.

of Th2 cytokines but not IFNγ, while memory Th1 cells produced large amounts of IFNγ but not Th2 cytokines. These results suggest that *in vivo* generated Th1 and Th2 memory cells preserved their original restricted cytokine production profiles. From these results, we decided to use KJ1$^+$ CD4 T cells recovered from BALB/c or BALB/c *nu/nu* recipient mice 4 weeks after cell transfer as *in vivo* generated memory CD4 T cells to investigate the molecular mechanisms that control the maintenance of memory Th2 cells.

Histone H3-K9/14 of the Th2 Cytokine Gene Loci Was Hyperacetylated in Memory Th2 Cells—We began with an assessment of the acetylation status of histones associated with the Th2 cytokine gene loci in freshly isolated *in vivo* generated memory Th2 cells. The KJ1$^+$ memory Th2 cells were isolated by cell sorting, and the acetylation levels of histone H3 (K9/14) was determined by ChIP assay as described previously (22). Histone H3-K9/14 associated with the *IL-4* and *IL-13*-related gene loci (CGRE, CNS1, V_A enhancer, IL-4p, and IL-13p) were hyperacetylated in both memory Th2 cells and effector Th2 cells compared with freshly isolated naïve DO11.10 TCR Tg CD4 T cells (Fig. 3*A*). The acetylation levels at the *IL-5* promoter were significantly lower in memory Th2 cells as compared with effector Th2 cells. No hyperacetylation in the *IFNγ* promoter was observed. A similar hyperacetylation pattern was observed in memory Th2 cells isolated 10 weeks after cell transfer (data not shown).

Next, *in vivo* generated memory Th1 and Th2 cells were prepared to examine the Th2-specific hyperacetylation (Fig. 3*B*). The levels of acetylation of the CGRE, CNS1, V_A enhancer, IL-4p and IL-13p region in memory Th2 cells were significantly higher than those of memory Th1 cells. Memory Th1 cells exhibited certain levels of acetylation of these regions. The acetylation levels of IL-5 in memory Th2 cells were equivalent to those of memory Th1 cells, but they were significantly higher than those of freshly prepared CD4T cells. Equivalent levels of acetylation in RAD50 promoter were seen. For the *IFNγ* promoter, there was no preferential increase in acetylation in the Th1 memory cells. We compared acetylation status of *IFNγ* promoter in effector and memory Th1 cells and found that significant levels of acetylation of the *IFNγ* promoter induced in effector Th1 cells were substantially decreased in memory Th1 cells (Supplemental Fig. 2). Taken together, these results suggest that memory Th1 and Th2 cells possess higher background levels of histone acetylation in all regions tested as compared with naïve T cells, and that Th2 memory cells preserved preferentially increased acetylation of histone H3-K9/14 in the *IL-4* and *IL-13* gene-related regions.

These results prompted us to examine whether a unique long-range Th2-specific histone hyperacetylation within the *IL-13* and *IL-4* loci (22) is preserved in memory Th2 cells. We analyzed the acetylation status of histone H3 in the *IL-13* and *IL-4* gene loci more precisely using 29 pairs of specific primers. Fig. 3*C* shows the actual ChIP assay PCR bands (Upper), the summary of relative band intensity (Ac-H3/Input DNA) and the ratios of acetylation intensity of effector and memory Th2 cells to that of freshly isolated CD4 T cells. The acetylation profiles induced in effector Th2 cells were maintained in memory Th2 cells with slightly decreased levels at the regions associated with IL-13. Furthermore, the boundary of Th2-specific hyperacetylation at the CGRE site was preserved in memory Th2 cells.

Histone H3 (K9/14) of the Th2 Cytokine Gene Loci Is Acetylated Equivalently in Effector and Central Memory Th2 Cells—Memory T cells can be subdivided into two distinct populations based on the expression level of CD62L (48). One is the effector memory T cell (CD44^{high}/CD62L^{low}) and the other is the central memory T cell (CD44^{high}/CD62L^{high}). The change in proportion of effector and central memory Th2 cells over time was assessed in our *in vivo* memory Th2 cell generation system (Supplemental Fig. 3*A*). The ratio (effector/central memory) in-

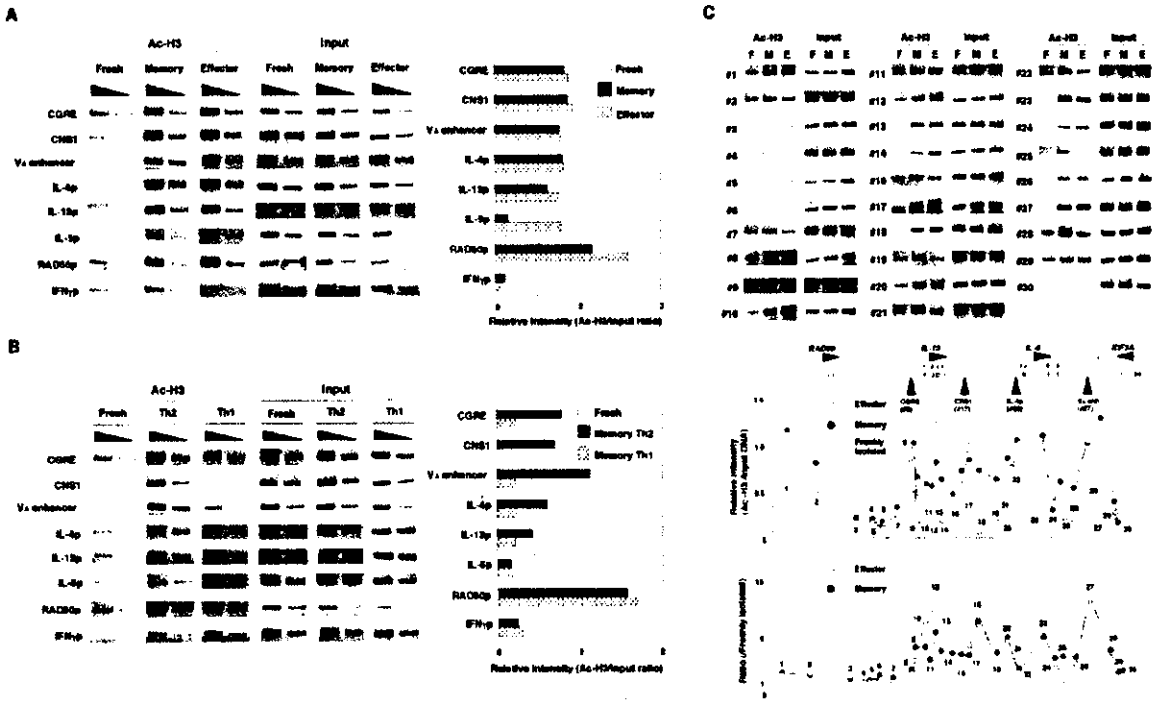

FIG. 3. **Acetylation status of histone H3-K9/14 in the Th2 cytokine gene loci in memory Th2 cells.** *A*, histone H3 (K9/14) acetylation of the Th2 cytokine gene loci in memory Th2 cells. *In vitro* differentiated effector Th2 cells were transferred into BALB/c *nu/nu* mice as in Fig. 1. Memory Th2 cells was prepared 4 weeks after cell transfer by sorting KJ1-positive cells. ChIP assay was performed with an anti-acetyl histone H3 (K9/14) antibody and the indicated specific primer pairs. PCR was performed with 3-fold serial dilution of template genomic DNA. Shown are the PCR product bands (*left*) and the relative intensity (*Ac-H3/Input*) for each primer pair (*right*). Three independent experiments with different T cell preparations were done with similar results. *B*, comparison of histone H3 acetylation of the Th2 cytokine gene loci between memory Th1 and Th2 cells. Shown are the PCR product bands (*left*) and the relative intensity (*Ac-H3/Input*) for each primer pair (*right*). Two independent experiments were performed with similar results. *C*, histone H3 hyperacetylation within the *IL-13* and *IL-4* loci in memory Th2 cells. Shown are the PCR product bands for each primer pair (*upper panel*), the relative intensity (*Ac-H3/Input*) (*middle panel*) and the Memory/Fresh or Effector/Fresh ratio (*lower panel*) of the band intensities. Three independent experiments with different T cell preparations were performed with similar results.

creased up to 4 weeks after cell transfer, and decreased thereafter. Phenotypic analysis revealed that these two memory Th2 subpopulations express similar levels of cytokine receptor components (IL-4Rα, Cγ, IL-2Rβ, and IL-7Rα) (Supplemental Fig. 3*B*). Both populations produced substantial amounts of IL-4, IL-5, and IL-13 with marginal production of IFNγ. The levels of IL-4 production were slightly but reproducibly higher in central memory Th2 cells, and those of IL-5 were higher in effector memory Th2 cells. The production of IL-13 was equivalent between these two subpopulations (Supplemental Fig. 3*C*, *lower left panel*).

Concurrently, we assessed the acetylation status of histone H3 (K9/14), and substantial and equivalent histone hyperacetylation of the IL-4 and IL-13-related regions were detected in these two subpopulations (Supplemental Fig. 3*D*). Similar results were obtained in effector and central memory Th2 cells 10 weeks after cell transfer (data not shown). These results would indicate that Th2-specific remodeled chromatin is preserved in both effector and central memory Th2 cells.

IL-4 Is Not Required for the Generation and the Maintenance of Memory Th2 Cells—IL-4 is a critical cytokine for the induction of chromatin remodeling of the Th2 cytokine gene loci during Th2 cell development. Consequently, we examined the requirement of IL-4 for the generation and the maintenance of memory Th2 cells. Splenic CD4 T cells from IL-4-deficient DO11.10 Tg mice with a BALB/c background were stimulated with OVA peptide and APC in the presence of exogenous IL-4 for 5 days. The effector Th2 cells from IL-4-deficient mice produced almost the same amounts of IL-5 and IL-13 compared with those from normal mice, and the acetylation status of the Th2 cytokine gene loci was almost equivalent (data not shown). Then, the cultured cells were transferred into recipient normal BALB/c mice. As shown in Fig. 4*A*, the numbers of KJ1$^+$CD4 T cells and the ratio of effector/central memory cells were similar between wild type (WT), IL-4$^{+/-}$ heterozygous (Hetero), and IL-4$^{-/-}$ homozygous deficient (KO) mice. Next, we used IL-4-deficient mice as hosts, and examined the generation of KJ1$^+$ cells. Equivalent levels of KJ1$^+$CD4 T cell generation were observed (Fig. 4*B*, *upper*). The ratio of effector/central memory cells was also similar regardless of the source donor cells or recipients, indicating the lack of dependence on IL-4 (Fig. 4*B*, *lower*).

The KJ1$^+$CD4 T cells generated in recipient mice shown in Fig. 4, *A* and *B* were purified by sorting, and their cytokine production profiles were determined by ELISA. The memory Th2 cells from IL-4-deficient mice produced equivalent amounts of IL-13, and slightly decreased levels of IL-5 (Fig. 4*C*). IFNγ production from IL-4-deficient memory Th2 cells was not robust but it was modestly increased (Fig. 4*C*, *extreme right panels*). IL-4 deficiency in the host mice did not affect the cytokine profiles of memory cells (Fig. 4*C*, *lower panels*). We assessed the acetylation status of histone H3 (K9/14) in the Th2 cytokine gene loci in the IL-4-deficient memory Th2 cells and found that the levels of acetylation in the *IL-4*-related gene loci (CGRE, CNS1, V_A enhancer, and IL-4p) were all equivalent among wild type and IL-4-deficient groups (Fig. 4*D*). The levels

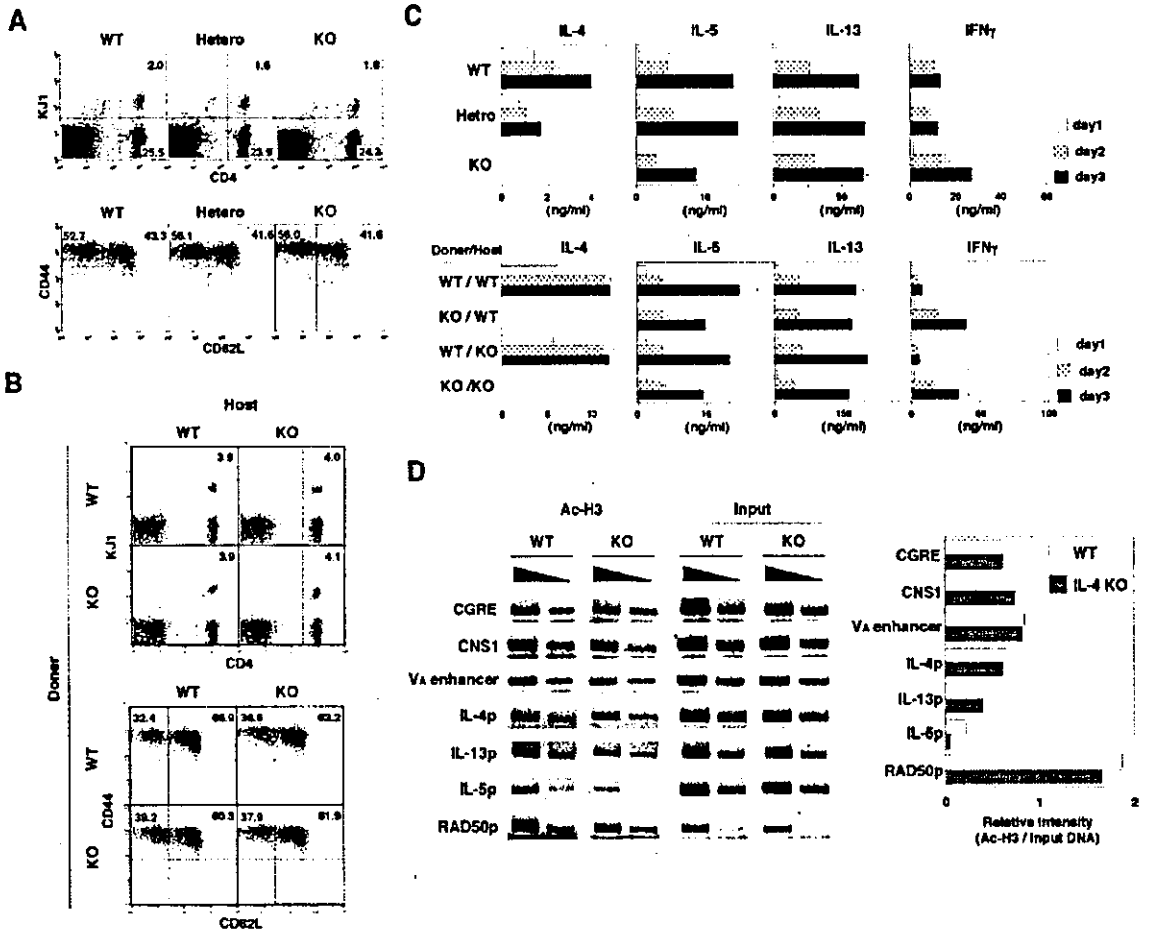

FIG. 4. **IL-4 is not required for the generation and the maintenance of memory Th2 cells.** *A*, *in vivo* generated Th2 cells were prepared from WT, IL-4$^{+/-}$ heterozygous (*Hetero*), and IL-4$^{-/-}$ homozygous-deficient (*KO*) mice 4 weeks after cell transfer into BALB/c mice. Representative staining profiles of CD4/KJ1 and CD62L/CD44 are shown with percentages in each quadrant. *B*, *in vivo* generated Th2 cells were prepared using WT or IL-4-deficient (KO) donor T cells, and WT and IL-4-deficient (KO) BALB/c recipient mice. *C*, effect of IL-4 deficiency on the cytokine production profiles of *in vivo* generated memory Th2 cells. Memory Th2 cells were generated as in *A* and *B*, restimulated with OVA peptide (1 μM), and the concentrations of cytokines in the culture supernatants were determined by ELISA. *D*, acetylation status of histone H3 of the Th2 cytokine gene loci in memory Th2 cells generated by transfer of IL-4-deficient effector Th2 cells. ChIP assay was performed as described in Fig. 3. PCR was performed with 3-fold serial dilution of template genomic DNA.

of acetylation at the *IL-13* promoter were slightly decreased in the absence of IL-4. The acetylation levels of the *IL-5* promoter was low in memory Th2 cells (see Fig. 3, *A* and *B*), and significantly lower in IL-4-deficient memory Th2 cells. These results indicate that IL-4 is not required for the generation of memory Th2 cells and the maintenance of the ability to produce Th2 cytokines. In addition, while IL-4 in T cells appears to play some specific role in the maintenance of acetylation at the *IL-5* gene locus, it does not affect the *IL-4*-related gene locus in memory Th2 cells. It may have some role in the maintenance of acetylation of the *IL-13*-related gene locus.

Memory Th2 Cells Express High Levels of GATA3 mRNA but Undetectable Amounts of GATA3 Protein—GATA3 is thought to be a master transcription factor and it is induced in developing Th2 cells in an IL-4- and STAT6-dependent manner. Since the Th2-specific acetylation profiles in the *IL-13* and *IL-4* gene loci were preserved in memory Th2 cell, we sought to examine the expression levels of GATA3 in memory Th2 cells. First, the expression of GATA3 mRNA was assessed by semi-quantitative RT-PCR analysis. The memory Th2 cells expressed substantial levels of GATA3 mRNA that were equivalent to those of effector Th2 cells (Fig. 5*A*). Two distinct promoters, *GATA3a* and original promoter *GATA3b* have been reported (49), and so we assessed the levels of mRNA of both sites in memory Th2 cells. GATA3a transcripts were detected only in the memory Th2 cells, although the levels were quite low when compared with GATA3b. The original *GATA3b* transcripts were detected in memory Th2 cells at equivalent levels to effector Th2 cells. The transcripts of the mature mRNA for IL-4, IL-5, and IL-13 were detected in effector Th2 cells but not in freshly isolated memory Th2 cells. Equivalent amounts of GATA3 mRNA were detected in wild-type and IL-4-deficient memory Th2 cells, suggesting that IL-4 is not required for the GATA3 transcription in memory Th2 cells (Fig. 5*B*). Similar results were obtained by real time PCR analyses (data not shown).

Next, the protein expression of GATA3 in memory Th2 cells was assessed by immunoblot analysis. Surprisingly, the expression levels of GATA3 protein in memory Th2 cells were very low (~1/10) and they were only equivalent to those of

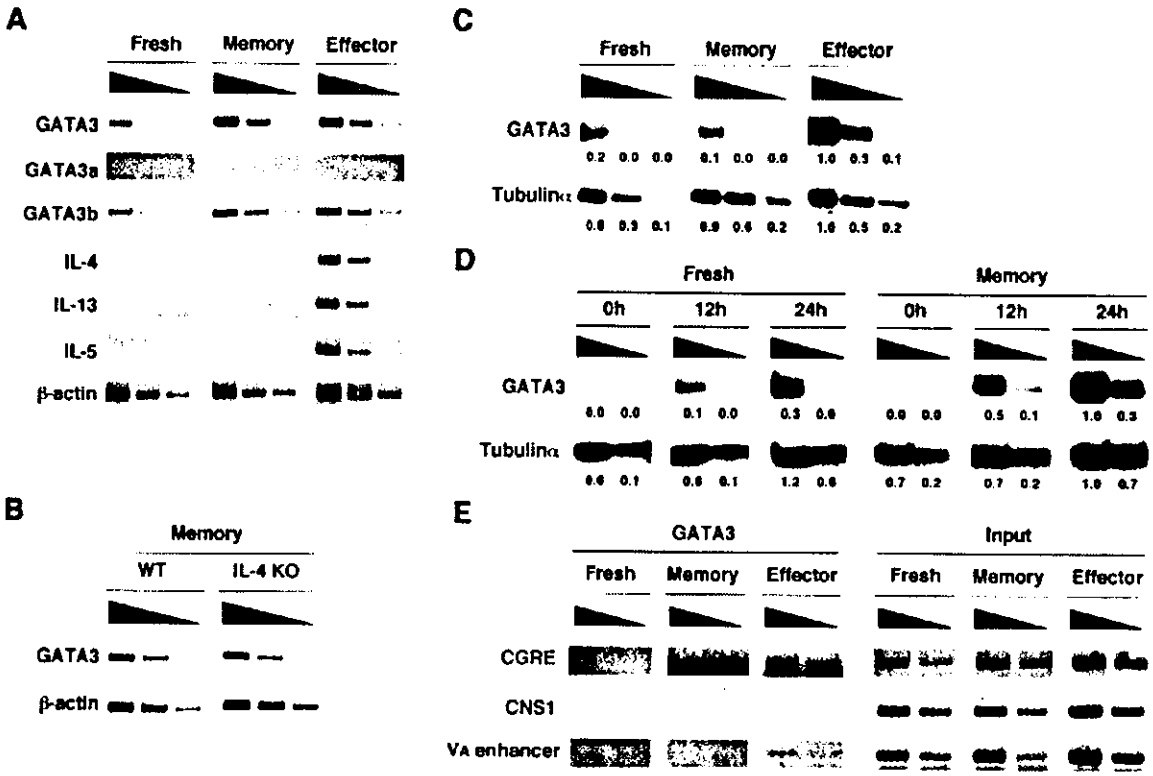

FIG. 5. **Expression of GATA3 mRNA and GATA3 protein in *in vivo* generated memory Th2 cells.** *A*, high level expression of GATA3 mRNA in memory Th2 cells. mRNA levels of GATA3, GATA3a, GATA3b, IL-4, IL-13, IL-5, and β-actin were determined by semiquantitative RT-PCR analysis with 3-fold serial dilutions of template cDNA. Shown are the representative PCR product bands of three independent experiments with memory Th2 cells generated in BALB/c *nu/nu* mice 4 weeks after cell transfer. *B*, IL-4-independent expression of GATA3 mRNA. The mRNA levels for GATA3 in IL-4-deficient memory Th2 cells were determined as described in *A*. *C*, expression of GATA3 protein in resting memory Th2 cells. Freshly prepared KJ1$^+$ CD4 T cells (*Fresh*), memory Th2 cells (*Memory*), and effector Th2 (*Effector*) were prepared as in *A*. The expression levels of GATA3 and tubulin-α protein were determined by immunoblotting. Arbitrary densitometric units are shown under each band. Three experiments were done with similar results. *D*, GATA3 protein induced in memory Th2 cells upon anti-TCR mAb restimulation. Freshly prepared KJ1$^+$ CD4 T cells and memory Th2 cells were stimulated with anti-TCR mAb under Th2-skewed conditions for indicated times. The expression levels of GATA3 and tubulin-α protein were examined by immunoblotting. *E*, GATA3 binding to the CGRE site was not detected in memory Th2 cells. ChIP assay using anti-GATA3 antibody was performed.

freshly prepared naïve CD4 T cells (Fig. 5*C*). However, 12 and 24 h after stimulation with anti-TCR mAb *in vitro*, memory Th2 cells expressed significantly higher amounts of GATA3 protein than freshly prepared naïve CD4 T cells (Fig. 5*D*). The efficient induction of GATA3 protein was also observed in IL-4-deficient memory Th2 cells upon anti-TCR mAb stimulation (data not shown). We reported previously the efficient binding of GATA3 protein to the CGRE regions in newly generated effector Th2 cells (22). Thus, we wanted to know whether the binding of GATA3 protein to the CGRE in memory Th2 cells in which histone hyperacetylation of the *IL-4* and *IL-13* gene loci was preserved. ChIP analyses with anti-GATA3 revealed that there was significant GATA3 binding to the CGRE region in effector Th2 cells but not in memory Th2 cells (Fig. 5*E*). No significant binding was observed at CNS1 and V_A enhancer regions in either memory or effector Th2 cells. Taken together, these results suggest that memory Th2 cells express substantial amounts of GATA3 mRNA although only marginal levels of GATA3 protein can be detected. Furthermore, histone hyperacetylation of the *IL-13* and *IL-4* gene loci appears to be maintained in a GATA3 protein expression-independent manner.

Intergenic Transcripts at the Downstream Region of the CNS1 Spanning to V_A Enhancer Site Are Preserved in Memory Th2 Cells—In our previous reports, we proposed a potential role of intergenic transcription for inducing long range histone hyperacetylation and the transactivation of the *IL-13* and *IL-4* gene loci (22, 25). Therefore, we assessed the intergenic transcripts of the *IL-13* and *IL-4* gene loci using 19 primer pairs (Fig. 6*A*). The ratios of band intensity (fresh/effector and memory/effector) in each group are summarized in the *lower panel* of Fig. 6*A*. In memory Th2 cells, substantial amounts of transcripts were detected in all regions that were tested, and their levels were essentially preserved at the downstream region of the CNS1 spanning to the V_A enhancer site. IL-4-deficient memory Th2 cells expressed equivalent amounts of intergenic transcripts at the CNS1, 18, V_A enhancer, and 28 sites as well. This indicates that IL-4 is not required for the intergenic transcription of these regions in memory Th2 cells (Fig. 6*B*).

Consequently, we assessed the changes in the intergenic transcript levels in memory Th2 cells after anti-TCR stimulation. The levels of intergenic transcripts upstream of the CNS1 region were increased substantially after anti-TCR stimulation, but those downstream of the CNS1 site remained unchanged (Fig. 6*C*). Also, there was no inhibition of the generation of intergenic transcripts in the presence of FK506, indicating that the intergenic transcripts were not dependent on the activation of calcineurin in memory Th2 cells. Under the same conditions, the mature IL-4 and IL-13 transcripts were

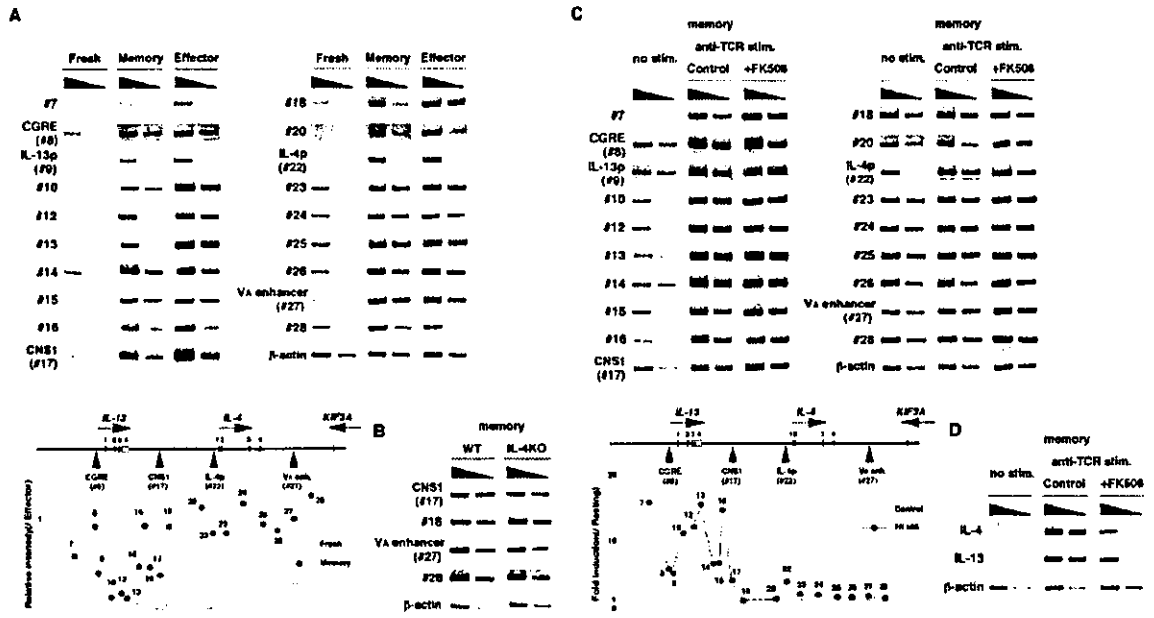

FIG. 6. **Intergenic transcripts are preserved in memory Th2 cells.** *A*, detection of non-coding intergenic transcripts of the *IL-13* and *IL-4* gene loci in memory Th2 cells. Freshly prepared KJ1$^+$ CD4 T cells (*Fresh*), memory Th2 cells (*Memory*), and effector Th2 (*Effector*) were prepared described in Fig. 5, and total RNA was prepared. To avoid contamination of genomic DNA, samples were treated with DNase I. Non-coding transcripts were determined by a semiquantitative RT-PCR analysis with 3-fold serial dilution of template cDNA. The ratios of band intensity of the fresh and memory cells to that of effector cells are depicted in the *lower panel*. Three independent experiments with different T cell preparations were performed with similar results. *B*, non-coding transcription in IL-4-deficient memory Th2 cells. The levels of intergenic transcription in IL-4-deficient memory Th2 cells were determined as described above. *C*, memory Th2 cells were prepared as in *A*, and stimulated with anti-TCR mAb for 48 h in the presence or absence of 100 nM of FK506. Non-coding transcripts were assessed as in *A*. The ratios of band intensity of cells after anti-TCR stimulation in the presence (*+FK506*) or absence (*Control*) of FK506 to that of before stimulation (*no stim.*) are summarized in the *lower panel*. *D*, levels of mature IL-4 and IL-13 transcripts in the cells as in *C*. Three independent experiments with different T cell preparations were performed with similar results.

induced by anti-TCR stimulation in memory Th2 cells, and these were found to be significantly inhibited in the presence of FK506 (Fig. 6*D*). These results suggest that the intergenic transcripts of the *IL-13* and *IL-4* gene loci were generated by a distinct signaling mechanism as compared with that for mature IL-13 and IL-4 mRNA.

Histone Methylation (H3-K4) in the Long Range Region of the IL-13 and IL-4 Gene Loci Is Totally Preserved in Memory Th2 Cells—It has been reported that the methylation of histone H3-K4 is well correlated with active chromatin in transcription and some specific role in the maintenance of H3-K9/14 acetylation in mammalian systems (50). Consequently, we analyzed the methylation status of histone H3-K4 of the *IL-4* and *IL-13* gene loci in fresh DO11.10 Tg KJ1$^+$ CD4 T cells (F), memory (M), and effector (E) Th2 cells using a series of primer pairs and anti-di- and tri-methyl histone specific Abs (Fig. 7*A*). The relative intensity profiles are depicted in Fig. 7*B*. The relative levels of di (Me2)- or tri (Me3)-methylation at histone H3-K4 of the *IL-4* and *IL-13* gene loci were low in fresh CD4 T cells, but there was substantial methylation at the site in memory Th2 cells and effector Th2 cells to almost equivalent levels. These results suggest that histone methylation (H3-K4) in the long range region of the *IL-13* and *IL-4* gene loci is totally preserved in memory Th2 cells.

Memory Th2 Cell-specific Accumulation of Pol II Complex at Specific Intergenic Regions (CNS1, IL-4p, and V_A Enhancer)—Because some of the histone methyltransferase for H3-K4 functionally interacted with Pol II (26), ChIP assay with anti-Pol II Ab was performed. Interestingly, strong bindings of Pol II to specific regions, *i.e.* CNS1 (17), *IL-4* promoter (22), and V_A enhancer (27) sites, and a weak binding to the CGRE site (8) were observed in memory Th2 cells (Fig. 7*C*). In addition, weak binding of Pol II was observed at almost all regions of the *IL-4* and *IL-13* gene loci in effector Th2 cells. Although nineteen regions throughout the *IL-13* and *IL-4* gene loci were analyzed, the strong binding of Pol II was observed at only these three sites in memory Th2 cells (Fig. 7*C*). We also tested additional 12 sites within the region, but found no additional strong sites (data not shown). The binding of TFIIB was observed at the same three strong binding sites for Pol II (CNS1, IL-4p, and V_A enhancer; Fig. 7*D*). These results indicate that highly restricted accumulation of Pol II complex to specific sites is unique to memory Th2 cells, and may play a role in the maintenance of intergenic transcription and histone methylation (H3-K4) in the *IL-13* and *IL-4* gene loci in memory Th2 cells.

DISCUSSION

In the present study, we investigated the molecular basis for the maintenance of Th2 cytokine production in memory Th2 cells using *in vivo* generated OVA-specific memory Th2 cells. These memory Th2 cells appeared to have typical memory Th2 cell phenotypes as evidenced by the prompt proliferation upon restimulation with a low dose antigen (Fig. 1*C*) and the production of large amounts of Th2-specific cytokines (Fig. 2).

It is known that IL-4-induced STAT6 activation and the subsequent induction of GATA3 protein are essential for chromatin remodeling including histone hyperacetylation in developing Th2 cells (22). In developed Th2 cells, the production of IL-4 and IL-13 is not dependent on IL-4 (51, 52). Here, we assessed the role for IL-4 in the generation and the maintenance of memory Th2 cells, and found that IL-4 is dispensable (Fig. 4). In addition, the expression of GATA3 protein may not

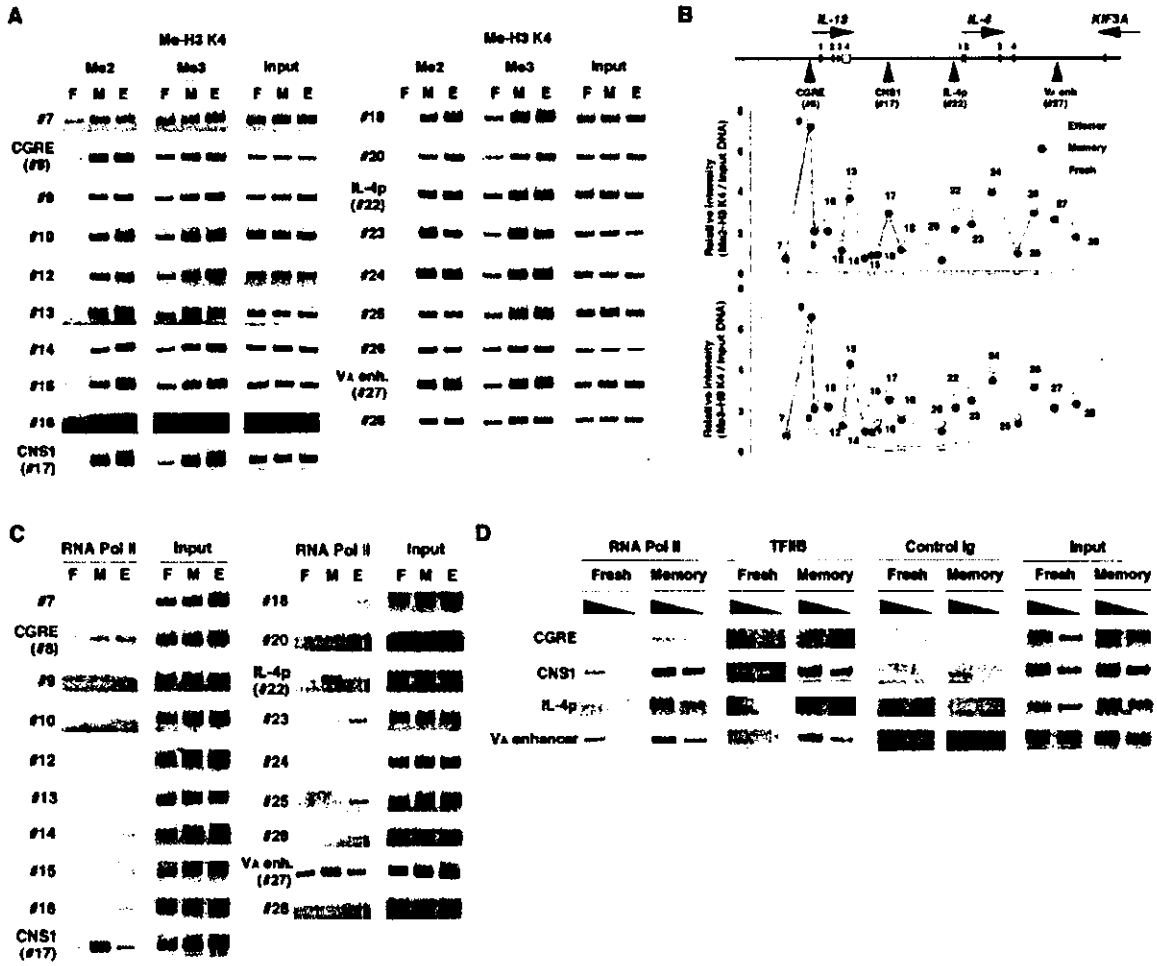

FIG. 7. **Histone methylation (H3-K4) in the long-range region of the *IL-13* and *IL-4* gene loci and accumulation of Pol II complex in memory Th2 cells.** *A* and *B*, histone H3 (*K4*) methylation of the *IL-13* and *IL-4* gene loci in memory Th2 cells. Anti-dimethyl- or anti-trimethyl-histone H3 (K4) antibodies and the indicated specific primer pairs were used. Shown are the PCR product bands for each primer pair (*A*) and Me2/Input (*B*, *upper*) and Me3/Input ratio (*B*, *lower*). Three independent experiments were done with similar results. *C*, binding of Pol II to highly restricted sites of the *IL-4* and *IL-13* gene loci in memory Th2 cells. ChIP assay was performed using anti-Pol II antisera and indicated specific primer pairs. *D*, ChIP assay was performed using anti-Pol II and anti-TFIIB antisera. PCR was performed with 3-fold serial dilution of template genomic DNA.

have an important role in the process because the protein expression level of GATA3 was marginal at best in the memory Th2 cells (Fig. 5*C*). However, our study revealed that the Th2-specific remodeled chromatin in the *IL-13* and *IL-4* gene loci was preserved in memory Th2 cells (Figs. 3 and 7, *A* and *B*). The upstream boundary of the hyperacetylation at the CGRE site and the levels of acetylation in each region assessed by a series of primer pairs were almost perfectly maintained (Fig. 3*C*). Thus, the molecular mechanisms that govern the maintenance of the remodeled chromatin in the *IL-13* and *IL-4* gene loci in memory Th2 cells appear to be distinct from those for the induction of chromatin remodeling.

As for the mechanisms responsible for the maintenance of remodeled chromatin, the transcriptional events including continuous intergenic transcription may play an important role (Fig. 6). The non-coding transcription of the *IL-13* and *IL-4* gene loci, particularly that of downstream regions of CNS1 was well preserved in memory Th2 cells, and it was insensitive to FK506 (Fig. 6*C*), suggesting that the non-coding regions are transcribed by a distinct mechanism from that for mature mRNA for IL-4 and IL-13. Interestingly, we identified highly restricted unique accumulation of Pol II complex at three intergenic regions (CNS1, IL-4p, and V_A enhancer) (Fig. 7, *C* and *D*). These are located in the region where the intergenic transcripts were perfectly preserved in memory Th2 cells (downstream of the CNS1 site), and thus this could account for the continuous generation of high level intergenic transcripts observed in the region. Similar highly restricted localization of Pol II within a locus control region was reported in the β-globin gene (53). As Pol II is known to associate with histone-modifying enzymes (26), Pol II localization within a locus control region may have also a specific role in histone modification, such as H3-K4 methylation and H3-K9/14 acetylation.

Site-specific histone methylation appears to play also an important role in transcriptional regulation (29). Methylation of H3-K4 disrupts binding of the nucleosome remodeling and deacetylase (NuRD) complex to H3 tails, thereby preventing targeted histone deacetylation catalyzed by the NuRD complex

(54, 55). The SET domain of MLL, a human homolog of *Drosophila trithorax*, is reported to be an H3-K4-specific methyltransferase, and the disruption of MLL SET domain reduced histone acetylation levels of the Hox *c8* gene locus in mouse embryo fibroblasts (50, 56). More recently, several groups have demonstrated that the yeast Set1 and Set2 H3-K4-specific methyltransferase complexes interact with Pol II (26). Thus, it is also probable that methylation of histone H3-K4 residues is important for the maintenance of the intergenic transcripts. Taken together, although we do not know the precise role of the accumulation of Pol II in a certain restricted regions at this time, intergenic transcription, methylation of histone H3-K4, and hyperacetylation of histone H3-K9/14 appear to be critical active events for maintaining the histone modification of the *IL-4* and *IL-13* gene loci in memory Th2 cells.

In contrast to the *IL-13* and *IL-4* gene loci, the level of histone hyperacetylation of the *IL-5* gene locus was dramatically decreased in memory Th2 cells as compared with those of effector Th2 cells (Fig. 3*A*). Also IL-4 dependence was observed in the histone hyperacetylation of the *IL-5* gene locus (Fig. 4*D*). Furthermore, di- and tri-methylation of H3-K4 was not observed at the *IL-5* locus in memory Th2 cells.[2] However, although the production of IL-5 after antigenic restimulation was slightly decreased in IL-4-deficient memory Th2 cells, substantial amounts of IL-5 were produced upon restimulation (Fig. 4C). The acetylation levels of histone H3 in the *IL-5* locus were rapidly increased after TCR restimulation in memory Th2 cells.[2] The kinetics of induction of histone acetylation of the *IL-5* gene locus appeared to correlate with the kinetics of the expression levels of GATA3 protein after anti-TCR stimulation (shown in Fig. 5*D*), suggesting that histone acetylation of the *IL-5* gene locus in memory Th2 cells remained highly dependent on GATA3. This suggests that the control mechanisms for the transcriptional memory of the *IL-5* gene are clearly distinct from that of the *IL-4* and *IL-13* gene loci. Similarly, hyperacetylation of the *IFN*γ promoter region was not preserved in memory Th1 cells (Fig. 3*B* and Supplemental Fig. 2). Further investigation is required to address the precise mechanisms that control the maintenance of remodeled chromatin of the *IL-5* and *IFN*γ gene loci in memory T cells.

Another unexpected but interesting result is that substantial levels of mRNA of GATA3 were detected in the freshly isolated memory Th2 cells (Fig. 5*A*). The transcription of GATA3 is maintained in the absence of IL-4 (Fig. 5*B*). These results indicated that the transcriptional induction of GATA3 in memory Th2 cells is independent on IL-4. Murphy and co-workers (57) reported that the expression of GATA3 is controlled by autoactivation. Two distinct promoters (*GATA3a* and *GATA3b*) control the expression of GATA3 (49). A newly identified promoter *GATA3a* is suggested to be responsible for GATA3-dependent *GATA3* transcription (GATA3 autoactivation). It is possible that the IL-4-independent transcription of *GATA3* in memory Th2 cells is mediated by GATA3 autoactivation. However, only trace levels of transcripts from the GATA3a were detected in memory Th2 cells (Fig. 5*A*) and the protein expression of GATA3 was marginal (Fig. 5*C*). Thus, the maintenance of GATA3 transcription in memory Th2 cells may not be explained by the action of the newly identified *GATA3a* promoter. Although the mechanism to account for the high level transcription of the *GATA3* gene in memory Th2 cells is not completely known, it appears to be clear that chromatin remodeling of the *GATA3* gene locus is induced during the Th2 cell differentiation and that it is maintained in the memory Th2 cells in an IL-4-independent manner. Furthermore, the protein expression level of GATA3 in memory Th2 cells was very low and comparable to those of naïve T cells (Fig. 5*C*), suggesting the presence of post-transcriptional regulation of GATA3 in memory Th2 cells. Following anti-TCR mAb restimulation of memory Th2 cells, the GATA3 protein expression is rapidly induced (Fig. 5*D*). This may account for the great amounts of Th2 cytokine production including IL-13 and IL-5 (Fig. 2), whose transcription is highly sensitive to GATA3 (58, 59).

Only weak association of Pol II was observed at the CGRE site, 71 bp of CGRE at 1.6-kbp upstream of the IL-13 locus exon 1 (Fig. 7*C*). We previously proposed that the CGRE plays a crucial role for GATA3-mediated targeting and downstream spreading of core histone hyperacetylation within the *IL-13* and *IL-4* gene loci in developing Th2 cells (22). The binding of Pol II to this site is dependent on GATA3 (22). Since GATA3 protein was not highly expressed in resting memory Th2 cells, Pol II may fail to associate CGRE site. However, histone H3-K4 was highly methylated at the CGRE site (Fig. 7*B*), suggesting that unique molecular events in chromatin of this particular region are taking place.

Memory CD4 T cells can be subdivided into two distinct subsets based on the expression level of CD62L (48). The $CD62L^{low}$ memory subset (effector memory) functionally resembles to effector cells that exhibit hyperresponsiveness to anti-CD3 and antigenic stimuli, high proliferative capacity, and rapid activation kinetics. The $CD62L^{high}$ memory subset (central memory) exhibits hyporeponsiveness to anti-CD3 and antigen stimuli, lower proliferative capacity, and slower activation kinetics (60). We have confirmed that the proliferative activity of the effector memory Th2 cells is higher than that of $CD62L^{high}$ central memory population.[2] We observed the $CD62L^{low}$ effector memory Th2 cells produced higher levels of IL-5 compared with $CD62L^{high}$ central memory Th2 cells in response to antigens, whereas IL-4 production was slightly lower and IL-13 production was equivalent (Supplemental Fig. 3*C*). Interestingly, the levels of histone H3-K9/14 acetylation of the *Th2* cytokine gene loci were equivalent between these two subpopulations (Supplemental Fig. 3). Although the acetylation status of histones in the *IL-13* and *IL-4* gene loci is not different, it will be of interest to explore the difference in the chromatin status of effector and central memory T cells.

In summary, memory Th2 cells maintain a unique Th2-specifc remodeled chromatin in the *IL-4* and *IL-13* gene loci, characterized by H3-K9/14 hyperacetylation and H3-K4 methylation associated with non-coding transcription and unique RNA Pol II accumulation in an IL-4-independent manner. The maintenance of the remodeled chromatin structure in the *IL-13* and *IL-4* gene loci in memory Th2 cells appears to be mediated by active molecular events that are distinct from those that operate during the induction of chromatin remodeling in developing Th2 cells.

Acknowledgments—We thank Dr. Ralph T. Kubo for helpful comments and constructive criticisms in the preparation of the manuscript. The authors also thank Kaoru Sugaya for excellent technical assistance.

[2] T. Nakayama and M. Yamashita, unpublished observation.

REFERENCES

1. Mosmann, T. R., and Coffman, R. L. (1989) *Adv. Immunol.* **46**, 111–147
2. Seder, R. A., and Paul, W. E. (1994) *Annu. Rev. Immunol.* **12**, 635–673
3. Reiner, S. L., and Locksley, R. M. (1995) *Annu. Rev. Immunol.* **13**, 151–177
4. Abbas, A. K., Murphy, K. M., and Sher, A. (1996) *Nature* **383**, 787–793
5. Constant, S. L., and Bottomly, K. (1997) *Annu. Rev. Immunol.* **15**, 297–322
6. O'Garra, A. (1998) *Immunity* **8**, 275–283
7. Gately, M. K., Renzetti, L. M., Magram, J., Stern, A. S., Adorini, L., Gubler, U., and Presky, D. H. (1998) *Annu. Rev. Immunol.* **16**, 495–521
8. Nelms, K., Keegan, A. D., Zamorano, J., Ryan, J. J., and Paul, W. E. (1999) *Annu. Rev. Immunol.* **17**, 701–738
9. Murphy, K. M., Ouyang, W., Farrar, J. D., Yang, J., Ranganath, S., Asnagli, H., Afkarian, M., and Murphy, T. L. (2000) *Annu. Rev. Immunol.* **18**, 451–494
10. Yamashita, M., Hashimoto, K., Kimura, M., Kubo, M., Tada, T., and

Nakayama, T. (1998) *Int. Immunol.* **10,** 577–591
11. Yamashita, M., Kimura, M., Kubo, M., Shimizu, C., Tada, T., Perlmutter, R. M., and Nakayama, T. (1999) *Proc. Natl. Acad. Sci. U. S. A.* **96,** 1024–1029
12. Yamashita, M., Katsumata, M., Iwashima, M., Kimura, M., Shimizu, C., Kamata, T., Shin, T., Seki, N., Suzuki, S., Taniguchi, M., and Nakayama, T. (2000) *J. Exp. Med.* **191,** 1869–1879
13. Grogan, J. L., and Locksley, R. M. (2002) *Curr. Opin. Immunol.* **14,** 366–372
14. Murphy, K. M., and Reiner, S. L. (2002) *Nat. Rev. Immunol.* **2,** 933–944
15. Zhang, D. H., Cohn, L., Ray, P., Bottomly, K., and Ray, A. (1997) *J. Biol. Chem.* **272,** 21597–21603
16. Zheng, W., and Flavell, R. A. (1997) *Cell* **89,** 587–596
17. Ouyang, W., Ranganath, S. H., Weindel, K., Bhattacharya, D., Murphy, T. L., Sha, W. C., and Murphy, K. M. (1998) *Immunity* **9,** 745–755
18. Lee, H. J., Takemoto, N., Kurata, H., Kamogawa, Y., Miyatake, S., O'Garra, A., and Arai, N. (2000) *J. Exp. Med.* **192,** 105–115
19. Lohning, M., Richter, A., and Radbruch, A. (2002) *Adv. Immunol.* **80,** 115–181
20. Ansel, K. M., Lee, D. U., and Rao, A. (2003) *Nat. Immunol.* **4,** 616–623
21. Turner, B. M. (2002) *Cell* **111,** 285–291
22. Yamashita, M., Ukai-Tadenuma, M., Kimura, M., Omori, M., Inami, M., Taniguchi, M., and Nakayama, T. (2002) *J. Biol. Chem.* **277,** 42399–42408
23. Avni, O., Lee, D., Macian, F., Szabo, S. J., Glimcher, L. H., and Rao, A. (2002) *Nat. Immunol.* **3,** 643–651
24. Fields, P. E., Kim, S. T., and Flavell, R. A. (2002) *J. Immunol.* **169,** 647–650
25. Omori, M., Yamashita, M., Inami, M., Ukai-Tadenuma, M., Kimura, M., Nigo, Y., Hosokawa, H., Hasegawa, A., Taniguchi, M., and Nakayama, T. (2003) *Immunity* **19,** 281–294
26. Hampsey, M., and Reinberg, D. (2003) *Cell* **113,** 429–432
27. Lachner, M., and Jenuwein, T. (2002) *Curr. Opin. Cell Biol.* **14,** 286–298
28. Sims, R. J., 3rd, Nishioka, K., and Reinberg, D. (2003) *Trends Genet* **19,** 629–639
29. Kouzarides, T. (2002) *Curr. Opin. Genet. Dev.* **12,** 198–209
30. Swain, S. L. (1994) *Immunity* **1,** 543–552
31. Sprent, J., and Surh, C. D. (2002) *Annu. Rev. Immunol.* **20,** 551–579
32. Swain, S. L., Hu, H., and Huston, G. (1999) *Science* **286,** 1381–1383
33. Tan, J. T., Ernst, B., Kieper, W. C., LeRoy, E., Sprent, J., and Surh, C. D. (2002) *J. Exp. Med.* **195,** 1523–1532
34. Polic, B., Kunkel, D., Scheffold, A., and Rajewsky, K. (2001) *Proc. Natl. Acad. Sci. U. S. A.* **98,** 8744–8749
35. Seddon, B., and Zamoyska, R. (2002) *J. Immunol.* **169,** 2997–3005
36. Dorfman, J. R., Stefanova, I., Yasutomo, K., and Germain, R. N. (2000) *Nat. Immunol.* **1,** 329–335
37. Lantz, O., Grandjean, I., Matzinger, P., and Di Santo, J. P. (2000) *Nat. Immunol.* **1,** 54–58
38. Jameson, S. C. (2002) *Nat. Rev. Immunol.* **2,** 547–556
39. Schluns, K. S., and Lefrancois, L. (2003) *Nat. Rev. Immunol.* **3,** 269–279
40. Kondrack, R. M., Harbertson, J., Tan, J. T., McBreen, M. E., Surh, C. D., and Bradley, L. M. (2003) *J. Exp. Med.* **198,** 1797–1806
41. Li, J., Huston, G., and Swain, S. L. (2003) *J. Exp. Med.* **198,** 1807–1815
42. Seddon, B., Tomlinson, P., and Zamoyska, R. (2003) *Nat. Immunol.* **4,** 680–686
43. Wu, C. Y., Kirman, J. R., Rotte, M. J., Davey, D. F., Perfetto, S. P., Rhee, E. G., Freidag, B. L., Hill, B. J., Douek, D. C., and Seder, R. A. (2002) *Nat. Immunol.* **3,** 852–858
44. Kopf, M., Le Gros, G., Bachmann, M., Lamers, M. C., Bluethmann, H., and Kohler, G. (1993) *Nature* **362,** 245–248
45. Murphy, K. M., Heimberger, A. B., and Loh, D. Y. (1990) *Science* **250,** 1720–1723
46. Kimura, M., Koseki, Y., Yamashita, M., Watanabe, N., Shimizu, C., Katsumoto, T., Kitamura, T., Taniguchi, M., Koseki, H., and Nakayama, T. (2001) *Immunity* **15,** 275–287
47. Rogers, P. R., Dubey, C., and Swain, S. L. (2000) *J. Immunol.* **164,** 2338–2346
48. Hengel, R. L., Thaker, V., Pavlick, M. V., Metcalf, J. A., Dennis, G., Jr., Yang, J., Lempicki, R. A., Sereti, I., and Lane, H. C. (2003) *J. Immunol.* **170,** 28–32
49. Asnagli, H., Afkarian, M., and Murphy, K. M. (2002) *J. Immunol.* **168,** 4268–4271
50. Milne, T. A., Briggs, S. D., Brock, H. W., Martin, M. E., Gibbs, D., Allis, C. D., and Hess, J. L. (2002) *Mol. Cell* **10,** 1107–1117
51. Hu-Li, J., Huang, H., Ryan, J., and Paul, W. E. (1997) *Proc. Natl. Acad. Sci. U. S. A.* **94,** 3189–3194
52. Huang, H., Hu-Li, J., Chen, H., Ben-Sasson, S. Z., and Paul, W. E. (1997) *J. Immunol.* **159,** 3731–3738
53. Johnson, K. D., Grass, J. A., Park, C., Im, H., Choi, K., and Bresnick, E. H. (2003) *Mol. Cell. Biol.* **23,** 6484–6493
54. Nishioka, K., Chuikov, S., Sarma, K., Erdjument-Bromage, H., Allis, C. D., Tempst, P., and Reinberg, D. (2002) *Genes Dev.* **16,** 479–489
55. Zegerman, P., Canas, B., Pappin, D., and Kouzarides, T. (2002) *J. Biol. Chem.* **277,** 11621–11624
56. Nakamura, T., Mori, T., Tada, S., Krajewski, W., Rozovskaia, T., Wassell, R., Dubois, G., Mazo, A., Croce, C. M., and Canaani, E. (2002) *Mol. Cell* **10,** 1119–1128
57. Ouyang, W., Lohning, M., Gao, Z., Assenmacher, M., Ranganath, S., Radbruch, A., and Murphy, K. M. (2000) *Immunity* **12,** 27–37
58. Zhang, D. H., Yang, L., and Ray, A. (1998) *J. Immunol.* **161,** 3817–3821
59. Lavenu-Bombled, C., Trainor, C. D., Makeh, I., Romeo, P. H., and Max-Audit, I. (2002) *J. Biol. Chem.* **277,** 18313–18321
60. Ahmadzadeh, M., Hussain, S. F., and Farber, D. L. (2001) *J. Immunol.* **166,** 926–935

Natural killer T cells accelerate atherogenesis in mice

Yukihito Nakai, Kazuya Iwabuchi, Satoshi Fujii, Naoki Ishimori, Nyambayar Dashtsoodol, Keiko Watano, Tetsuya Mishima, Chikako Iwabuchi, Shinya Tanaka, Jelena S. Bezbradica, Toshinori Nakayama, Masaru Taniguchi, Sachiko Miyake, Takashi Yamamura, Akira Kitabatake, Sebastian Joyce, Luc Van Kaer, and Kazunori Onoé

We have investigated the potential role of CD1d-restricted natural killer T (NKT) cells in the development of atherosclerosis in mice. When fed an atherogenic diet (AD), NKT cell–deficient CD1d$^{-/-}$ mice had significantly smaller atherosclerotic lesions than AD-fed C57BL/6 (wild-type [WT]) mice. A significant reduction in atherosclerotic lesions was also demonstrated in AD-fed, low-density lipoprotein receptor–deficient (Ldlr$^{-/-}$) mice reconstituted with CD1d$^{-/-}$ bone marrow cells compared with the lesions observed in Ldlr$^{-/-}$ mice reconstituted with WT marrow cells. In addition, repeated injections of α-GalCer or the related glycolipid OCH to apolipoprotein E knockout (apoE$^{-/-}$) mice during the early phase of atherosclerosis significantly enlarged the lesion areas compared with mice injected with vehicle control. However, administering α-GalCer to apoE$^{-/-}$ mice with established lesions did not significantly increase the lesion area but considerably decreased the collagen content. Atherosclerosis development in either AD-fed WT or apoE$^{-/-}$ mice was associated with the presence of Vα14Jα18 transcripts in the atherosclerotic arterial walls, indicating that NKT cells were recruited to these lesions. Thioglycolate-elicited macrophages pulsed with oxidized low-density lipoproteins expressed enhanced CD1d levels and induced NKT cells to produce interferon-γ, a potentially proatherogenic T-helper 1 (T_H1) cytokine. Collectively, we conclude that NKT cells are proatherogenic in mice. (Blood. 2004;104:2051-2059)

Introduction

Atherosclerosis is an inflammatory vascular disease that involves components of the innate and acquired immune systems.[1-3] Several studies have suggested that lymphocytes, which are detected in atherosclerotic lesions in humans and mice,[4,5] play a proatherogenic role.[6-8] Recently, the role of distinct lymphocyte subsets in the development of atherosclerosis has been evaluated. For example, emerging evidence indicates that T-helper 1 (T_H1) cells are proatherogenic,[9] whereas T_H2 cells are antiatherogenic.[10,11] These observations are further supported by the finding that T_H1 cytokines (eg, interferon-γ [IFN-γ and interleukin-12 [IL-12]) are important in the progression of atherosclerosis[12-15] and that, among T_H2 cytokines, IL-10 is antiatherogenic.[16] On the other hand, recent studies have suggested that B cells play a protective role in atherogenesis.[17,18]

Natural killer T (NKT) cells are a unique subset of lymphocytes that have surface markers and functions of T cells and NK cells.[19-23] Several characteristics of NKT cells suggest that they may play a role in the atherogenic process. Most NKT cells express an invariant Vα14Jα18 T-cell receptor (TCR)–Vα chain paired with a restricted set of TCR-Vβ chains. These classical NKT cells recognize lipid antigens presented by the major histocompatibility complex (MHC) class I–like molecule CD1d, produce copious amounts of IFN-γ and IL-4 on activation,[22] and constitutively express Fas-ligand.[23] Moreover, NKT cells play a protective role in several autoimmune diseases, infections, and tumor progression/metastasis.[20] Protective effects of NKT cells and their ligands in autoimmunity are largely attributed to their capacity to promote T_H2 immune responses.[24,25] However, in some situations, NKT cells can contribute to the development of T_H1 immune responses as well.[26] Therefore, it was difficult to predict whether NKT cells would play a proatherogenic or an antiatherogenic role.[2]

To date, few studies have investigated the role of CD1d and CD1d-dependent T cells in atherogenesis. CD1d-expressing cells are present in human atherosclerotic plaques,[27] suggesting that NKT cells may be recruited to the lesions. Furthermore, treatment of apolipoprotein E knockout (apoE$^{-/-}$) mice,[28] a model of severe

From the Division of Immunobiology, Research Section of Pathophysiology, Institute for Genetic Medicine, Hokkaido University, Sapporo; the Department of Cardiovascular Medicine, Graduate School of Medicine, Hokkaido University, Sapporo; the Laboratory of Molecular and Cellular Pathology, Graduate School of Medicine, Hokkaido University, Sapporo; the Department of Immunology, Graduate School of Medicine, Chiba University; the Laboratory of Immune Regulation, Rikagaku Kenkyusho (RIKEN) Institute of Physical and Chemical Research, Research Center for Allergy and Immunology, Yokohama; the Department of Immunology, National Institute of Neuroscience, NCNP, Kodaira, Japan; the Department of Microbiology and Immunology, School of Medicine, Vanderbilt University, Nashville, TN; and The Jackson Laboratory, Bar Harbor, ME.

Submitted October 14, 2003; accepted March 31, 2004. Prepublished online as *Blood* First Edition Paper, April 27, 2004; DOI 10.1182/blood-2003-10-3485.

Supported in part by Grant-in-Aid for Scientific Research S and B, Grant-in-Aid for Exploratory Research from the Ministry of Education, Culture, Science, Sports and Technology, Japan (K.O., S.F., K.I.); by grants from the Noastec Foundation (K.I., S.F., A.K., K.O.), the Mochida Memorial Foundation for Medical and Pharmaceutical Research (K.I.), the Akiyama Foundation (K.I., Y.N., T.M., C.I.), Daiwa Securities Health Foundation (K.I., C.I., K.N., S.F.), the Suhara Memorial Foundation (K.I., Y.N., N.D., C.I., S.F.), and the Program for the Promotion of Fundamental Studies in Health Sciences of the Pharmaceutical and Medical Devices Agency (T.Y.); and by National Institutes of Health grants AI50953, NS44044, HL68744 (L.V.K.), and AI42284 (S.J.).

Reprints: Kazuya Iwabuchi or Kazunori Onoé, Division of Immunobiology, Research Section of Pathophysiology, Institute for Genetic Medicine, Hokkaido University, Kita-15 Nishi-7, Kita-ku, Sapporo 060-0815, Japan; e-mail: akimari@igm.hokudai.ac.jp; kazunori@igm.hokudai.ac.jp.

The publication costs of this article were defrayed in part by page charge payment. Therefore, and solely to indicate this fact, this article is hereby marked "advertisement" in accordance with 18 U.S.C. section 1734.

atherosclerosis, with lipopolysaccharide (LPS) resulted in NKT cell recruitment to the atherosclerotic plaques.[29] However, whether NKT cells are directly involved in the development or the regulation of atherosclerosis remains to be investigated.

In the present study, we compared atherosclerotic lesions induced by an atherogenic diet (AD) between NKT cell–deficient $CD1d^{-/-}$[30] and wild-type C57BL/6 (WT) mice and between low-density lipoprotein receptor–deficient ($Ldlr^{-/-}$) mice[31] reconstituted with bone marrow (BM) cells from $CD1d^{-/-}$ mice and $Ldlr^{-/-}$ mice reconstituted with BM of WT mice. Moreover, we examined whether NKT cell ligands (α-galactosylceramide[32] (α-GalCer) and OCH[33]) could modulate atherogenesis in $apoE^{-/-}$ mice. Our findings consistently demonstrated that NKT cells played a proatherogenic role. Possible mechanisms underlying the proatherogenic role of NKT cells are discussed.

Materials and methods

Glycolipids

α-GalCer (Pharmaceutical Research Laboratories, Kirin Brewery, Gunma, Japan) and OCH were dissolved in either 0.5% polysorbate-20 at 220 μg/mL or dimethyl sulfoxide at 100 μg/mL, respectively, and were further diluted with phosphate-buffered saline (PBS) before use.

Mice

Female WT (Japan SLC, Hamamatsu, Japan), $CD1d^{-/-}$[30] (Vanderbilt University, Nashville, TN), $Jα18^{-/-}$[34] (Chiba University, Chiba, Japan), $Ldlr^{-/-}$, and $apoE^{-/-}$ (The Jackson Laboratory, Bar Harbor, ME) mice with the C57BL/6 genetic background were used throughout the study. WT and $CD1d^{-/-}$ mice were fed a regular chow diet or the atherogenic diet (AD) (15% fat, 1.25% cholesterol, and 0.5% cholic acid; Nihon-nohsan, Yokohama, Japan) from 10 to 30 weeks of age. All animal care and experimental procedures conformed to the regulations of the Committee of Hokkaido University on Animal Experimentation.

BMT

Bone marrow transplantation (BMT) was performed with lethally irradiated (9.5 Gy) $Ldlr^{-/-}$ mice as recipients, as previously described.[35] Briefly, recipient mice were injected with T cell–depleted BM cells (5×10^6) from WT mice (Thy1.1 in BMT protocol, referred to as [WT→$Ldlr^{-/-}$]), $CD1d^{-/-}$ mice ([$CD1d^{-/-}$→$Ldlr^{-/-}$]), or $Ldlr^{-/-}$ mice ([$Ldlr^{-/-}$→$Ldlr^{-/-}$]). Treated mice were administered oxytetracyclin (Pfizer Japan, Tokyo, Japan) in drinking water for 4 weeks and then placed on the AD for 5 weeks. Reconstitution was assessed by evaluating thymocyte expression of CD1d for $CD1d^{-/-}$ donors and both Thy1.1 (donor) and Thy1.2 (recipient) for WT donors using flow cytometry.

Induction of atherosclerotic lesions

Early-phase studies. $ApoE^{-/-}$ mice were divided into 4 groups (n = 10 each): 1 group received intraperitoneal (intraperitoneal) injections of 0.1 μg/g body weight (BW) α-GalCer; 1 group received its vehicle; and the remaining groups were administered 0.3 μg/g BW OCH or its vehicle, respectively. Injections were started at 8 weeks of age and repeated every 2 weeks. At 13 weeks of age, mice were killed and used for experiments. Blood samples were consecutively collected from the retro-orbital plexus at 0, 2, 5, 12, 24, 48, and 72 hours after injection of either α-GalCer or OCH, and the levels of IFN-γ and IL-4 were quantitated using enzyme-linked immunosorbent assay (ELISA; Biosource, Camarillo, CA).

Late-phase studies. Ten mice received intraperitoneal injections of 0.1 μg/g BW α-GalCer or vehicle every week starting from 8 weeks of age. One week after the eleventh injection, mice were killed and used for experiments.

Serum chemistry

Amounts of total cholesterol, high-density lipoprotein (HDL) cholesterol, and triglyceride concentrations in sera were determined with colorimetric assay kits (Kyowa Medex, Tokyo, and Serotekku, Sapporo, Japan). Individual serum alanine aminotransferase and total bilirubin were quantitated using the Fuji Drychem system (Fujifilm Medical, Osaka, Japan).

Quantitative analyses of atherosclerotic lesion areas

Atherosclerotic lesions were analyzed as previously described.[35] In brief, the basal portion of the heart and proximal aortic root were excised and embedded in OCT compound and frozen in liquid nitrogen. Eight serial cryosections of 10-μm thickness at 80-μm intervals throughout the aortic sinus were stained with oil red O (Sigma, St Louis, MO) and hematoxylin. Lesion images were captured with an Olympus BX50 microscope (Tokyo, Japan) equipped with a Fujix HC-300Z/OL digital camera (Fijifilm, Kanagawa, Japan) and Photograb-300 SH-3 software (Fujifilm). Captured images were further analyzed with Scion Image software (Scion, Frederick, MD). For advanced lesions, the entire aorta was examined using the en face method, as described elsewhere.[36]

Characterization of atherosclerotic lesions

Immunohistochemistry was performed on 8-μm thick cryosections, as previously described.[37] Rat monoclonal antibodies (mAbs) to mouse macrophages (MOMA-2; Serotec, Oxford, United Kingdom), hamster antimouse CD3 (BD Biosciences, San Jose, CA), anti–α-smooth muscle actin (DAKO, Glostrup, Denmark), rat antimouse IFN-γ (BioSource), rat antimouse IL-10 (Endogen, Woburn, MA), biotinylated secondary antibodies to the respective primary reagents, and streptavidin–horseradish peroxidase (DAKO) were used for detection. Signals were developed with DBA kits (Vector Laboratories, Burlingame, CA). The number of $CD3^+$ cells per cross-section of lesion area was counted at × 400 magnification. Elastica-Masson staining was performed to analyze the composition of the lesion using 3 aortic cross-sections per animal from 10 animals. The percentage of collagen-rich matrix areas among the total lesion areas was defined as collagen contents. Total cell numbers per lesion were also counted.

RT-PCR

WT (fed the chow diet or the AD), $apoE^{-/-}$, and $Jα18^{-/-}$ mice were killed after overnight fasting. After whole body perfusion with cold RNase-free PBS, aortae from the ascending portion to the end of the thoracic aorta were removed, dissected longitudinally, and washed meticulously in cold PBS to remove attached hematocytes and tissue fragments outside the aortae. RNA extraction and reverse transcription–polymerase chain reaction (RT-PCR) were performed as described previously.[38]

Flow cytometry

Splenocytes were prepared by lysing red blood cells with Tris-NH_4Cl solution. Hepatic mononuclear cells (HMNCs) were isolated using 33% Percoll (Amersham Pharmacia Biotech, Piscataway, NJ), as previously reported.[39] Cells were incubated with 2.4G2 mAb (anti-FcγR) to block nonspecific staining and were stained with a combination of the following mAb conjugates: for lymphocytes—biotinylated anti-Thy1.1 (OX7), fluorescein isothiocyanate (FITC) anti-Thy1.2 (Coulter, Miami, FL), anti-CD1d (1B1), anti-TCRβ (H57-597), and phycoerythrin (PE) anti-NK1.1 (PK136) (all from BD Biosciences, except Thy1.2); for macrophages—biotinylated anti-H-$2K^b$ (AF6-88.5), anti-I-A^b (AF6-120.1), anti-CD40 (3/23), and antimouse (BALB/c) immunoglobulin G2aκ (IgG2aκ) (G155-178; BD Biosciences), FITC anti-CD1d (1B1) and -rat IgG2b (LODNP57; Immunotech, Marseille, France), and PE anti–Mac-1 (CL8941; Cedarlane, Hornby, Ontario, Canada). Streptavidin-allophycocyanin (APC) (BD Biosciences) was used for detection of biotinylated mAb. Mouse CD1d/α-GalCer tetramers were prepared as previously described.[40] Cells were incubated with FITC anti-TCRβ and PE anti-NK1.1 and then with APC α-GalCer–loaded CD1d tetramers. Propidium iodide (Sigma) positive cells were

electronically gated out from the analysis, and stained cells were analyzed using a FACSCalibur flow cytometer, as described elsewhere.[38]

In vitro culture of splenocytes from AD- or chow-fed WT mice treated with α-GalCer

Splenocytes were obtained from either AD- or chow-fed WT mice 2 to 12 hours after intravenous injection with 0.1 μg/g BW α-GalCer. Cells were suspended in RPMI 1640 supplemented with 10% fetal calf serum, 100 U/mL penicillin, 100 μg/mL streptomycin, and 5×10^{-5} M 2-mercaptoethanol (culture medium) and were cultured in 24-well plates at 5×10^6/mL for 1.5 hours without additional stimulation. Culture supernatants were harvested and quantitated for IL-4 levels with ELISA kits (Biosource) and for IFN-γ and IL-10 with Cytometric Bead Array kits (BD Biosciences) by flow cytometry, according to the manufacturer's instructions.

Response of HMNCs to oxidized low-density lipoprotein in vitro

Peritoneal cells were harvested from young WT or CD1d$^{-/-}$ mice 4 days after intraperitoneal injection of 4.05% thioglycolate. Cells were suspended at a concentration of 2×10^6/mL in culture medium, incubated at 37°C for 24 to 48 hours with LDL, oxidized LDL (OxLDL) (10 and 50 μg/mL; Biomedical Technologies, Stoughton, MA), or vehicle alone, and used for flow cytometric analysis. For cytokine analysis, the peritoneal cells (2×10^5/well) were cultured in 96-well plates at 37°C for 2 hours and were washed to remove nonadherent cells. Adherent cells were incubated at 37°C for 48 hours with LDL or OXLDL. After incubation, each well was washed 3 times, and the adherent macrophages were irradiated with 30 Gy x-rays. HMNCs isolated from WT mice (2×10^5/well) were cultured with these macrophages in the presence of recombinant human IL-2 (1000 U/mL; Takeda Chemical Industries, Osaka, Japan) for 24 hours. The supernatant was quantitated for IFN-γ and IL-4 levels with ELISA kits (Biosource).

Statistical analysis

Results were expressed as mean ± SE. Statistical analysis was performed using the Student t test or the Mann-Whitney U rank sum test. All data analyses were performed using Statview software (Abacus Concepts, Berkeley, CA). Values with $P < .05$ were considered statistically significant.

Results

Development of atherosclerotic lesions in CD1d$^{-/-}$ mice

WT (n = 20) and CD1d$^{-/-}$ (n = 18) mice were fed on the AD for 20 weeks. All mice on the AD appeared generally to be in good health throughout the study except for the development of diet-induced liver steatosis and its consequential liver damage. When the sizes of atherosclerotic lesions in aortae were compared, the lesions in CD1d$^{-/-}$ mice were smaller than those in WT mice (Figure 1A). Mean lesion areas in CD1d$^{-/-}$ mice (2292 ± 397 μm^2) were significantly smaller than those in WT mice (5627 ± 580 μm^2) ($P = .014$) (Figure 1B). These findings demonstrate that CD1d deficiency reduces atherosclerotic lesions. Concerning serum lipid profiles, total cholesterol, HDL cholesterol, and triglyceride levels were not significantly different between WT (137.9 ± 8.0 mg/dL, 36.3 ± 1.6 mg/dL, and 57.5 ± 3.4 mg/dL, respectively) and CD1d$^{-/-}$ (140.2 ± 14.7 mg/dL, 38.1 ± 2.4 mg/dL, and 59.9 ± 4.4 mg/dL, respectively) mice. Histologic findings of liver sections stained with hematoxylin and eosin revealed typical steatosis to similar extents for WT and CD1d$^{-/-}$ mice fed on the AD (data not shown). Serum alanine aminotransferase and total bilirubin levels in WT and CD1d$^{-/-}$ mice also decreased within similar levels (WT, 111.3 ± 6.9 U/L, 0.6 ± 0.1 mg/dL; CD1d$^{-/-}$, 108.2 ± 14.5 U/L, 0.6 ± 0.1 mg/dL).

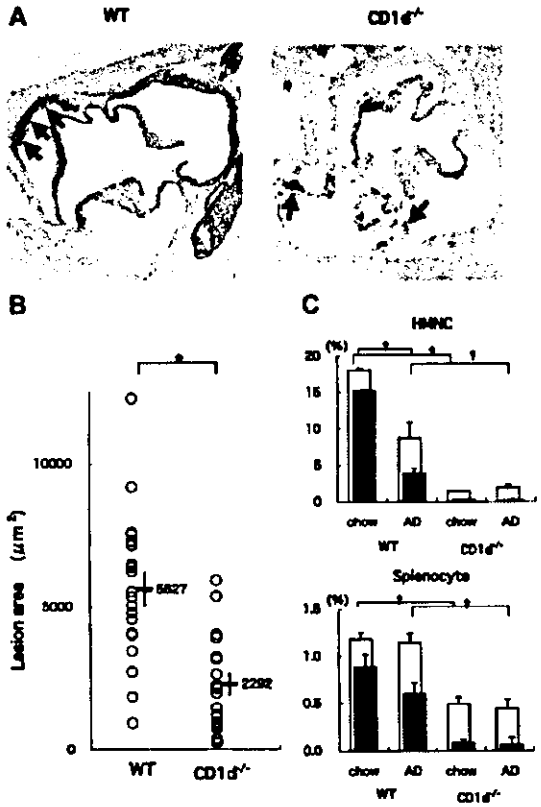

Figure 1. Atherosclerotic lesion areas in WT and CD1d$^{-/-}$ mice fed on the AD. (A) Representative histologic sections of WT and CD1d$^{-/-}$ mice fed on the AD. Arrows represent the oil red O–positive atherosclerotic lesions typically observed within the internal elastic lamina (original magnification, × 40). (B) Mean lesion areas of WT and CD1d$^{-/-}$ mice. Each symbol represents the lesion area of an individual mouse. Horizontal bars and numbers represent the mean of all mice within each group, and vertical bars represent SEM. (C) Prevalence of NKT cells in WT and CD1d$^{-/-}$ mice. HMNCs and splenocytes were prepared and stained with FITC anti-TCRαβ, PE anti-NK1.1, and APC-CD1d/α-GalCer tetramer, as described in "Materials and methods." Open columns represent the proportion of total NKT cells, and closed columns represent the proportion of CD1d/α-GalCer tetramer$^+$ cells. Each value represents the mean ± SE calculated from more than 5 experiments. Statistical analyses were performed with the Mann-Whitney U test. †$P < .01$ (for closed columns and open columns); *$P < .05$.

Flow cytometric analyses of NKT cells

Using flow cytometry, we analyzed NKT cells in the liver, spleen, and peripheral blood of WT mice fed either the chow diet or the AD. NK1.1$^+$TCRβ^{int} (ie, NKT) cells represented 18.1% ± 2.6% of the HMNCs of WT mice on the chow diet (Figure 1C, top panel). Among NK1.1$^+$TCRβ^{int} cells, 84.2% ± 4.1% stained with α-GalCer–loaded CD1d tetramers. It should be noted that the mean proportion of total NK1.1$^+$TCRβ^{int} cells in HMNCs of AD-fed WT mice (8.7% ± 2.3%) was significantly lower than that in chow-fed WT mice ($P = .009$). This was attributed to the considerable reduction of CD1d/α-GalCer tetramer$^+$ cells in AD-fed mice. Proportions of CD1d/α-GalCer tetramer$^-$ cells remained unaltered among chow- and AD-fed animals. Similarly, a mild reduction in the prevalence of tetramer$^+$ NKT cells among splenocytes of AD-fed mice was noted (Figure 1C, bottom panel; $P = .07$), but the proportion of total NK1.1$^+$TCRβ^{int} cells was unchanged. In CD1d$^{-/-}$ mice, the proportion of NK1.1$^+$TCRβ^{int} HMNCs was markedly smaller than that in WT mice, and tetramer$^+$ cells were not detected. Of note, the proportion of NK1.1$^+$TCRβ^{int} cells in CD1d$^{-/-}$ mice was unaffected by

AD feeding (1.5% ± 0.3% on the chow diet compared with 1.9% ± 0.4% on the AD). Similar results were obtained with splenocytes of $CD1d^{-/-}$ mice. No significant changes were seen in conventional T-cell subsets ($CD4^+$, $CD8^+$), γδ T cells, and NK cells by AD feeding in WT and $CD1d^{-/-}$ mice (data not shown).

Production of cytokines by splenocytes from AD- or chow-fed WT mice treated with α-GalCer

Our results indicate that AD feeding quantitatively and qualitatively alters the Vα14 NKT cell population of WT mice. One hallmark of NKT cells is their capacity to rapidly produce cytokines on TCR engagement.[22,41] To examine whether AD feeding influences the functional status of NKT cells, we administered a synthetic glycolipid, α-GalCer, to AD- or chow-fed WT mice, and 2 or 12 hours later we measured the amounts of IFN-γ, IL-4, and IL-10 produced by splenocytes in vitro. Two hours after α-GalCer injection, IFN-γ levels were significantly higher in AD-fed WT splenocytes than in chow-fed WT splenocytes ($P = .034$) (Figure 2). In contrast, IL-4 and IL-10 levels were significantly lower in AD-fed WT splenocytes than in chow-fed WT splenocytes ($P = .021$, $P = .047$, respectively). At 12 hours, IFN-γ levels were slightly higher in AD-fed WT splenocytes ($P = .094$), amounts of IL-4 decreased to undetectable levels in both groups, and IL-10 levels were still significantly lower in AD-fed WT splenocytes ($P = .009$). Experiments using HMNCs from AD- and chow-fed WT mice showed similar results (data not shown). Because NKT cells (particularly CD1d/α-GalCer tetramer$^+$ NKT cells) were decreased in AD-fed WT mice (Figure 1C), these findings indicate that NKT cells in AD-fed WT mice exhibit an enhanced capacity to produce cytokines, especially IFN-γ. It should be noted that AD feeding of WT mice shifted the cytokine production pattern in response to α-GalCer stimulation toward a T_H1 profile. Importantly, it has been reported that T_H1 responses are proatherogenic.[10-14]

Development of atherosclerosis in $Ldlr^{-/-}$ mice reconstituted with BM cells from $CD1d^{-/-}$ or WT mice

Next, to examine whether NKT cell deficiency is directly related to the reduction of atherosclerotic lesions, [WT→$Ldlr^{-/-}$] and [$CD1d^{-/-}$→$Ldlr^{-/-}$] BM chimeric mice (n = 7 in each group) were prepared. Four weeks after BMT, almost all thymocytes from [$CD1d^{-/-}$→$Ldlr^{-/-}$] chimeras used in these experiments were $CD1d^-$ and, thus, of donor origin (Figure 3A). In addition, thymocytes from [WT→$Ldlr^{-/-}$] chimeras were mostly $Thy1.1^+$ (donor) (donor chimerism = 99.0% ± 0.81%). AD feeding for 5 weeks led to similar levels of hypercholesterolemia in both groups (total cholesterol or HDL cholesterol, [WT→$Ldlr^{-/-}$]: 2147 ± 144 mg/dL or 15.0 ± 3.5 mg/dL; [$CD1d^{-/-}$→$Ldlr^{-/-}$]: 2207 ± 119 mg/dL or 15.9 ± 1.6 mg/dL, respectively). However, the atherosclerotic lesions in [$CD1d^{-/-}$→$Ldlr^{-/-}$] mice were significantly smaller than those in [WT→$Ldlr^{-/-}$] mice (Figure 3C-D). Immunohistochemistry revealed that the main components of the lesions were MOMA-2^+ macrophages in both groups (Figure 3E, upper). Notably, $CD3^+$ cells were significantly more abundant in [WT→$Ldlr^{-/-}$] mice than in [$CD1d^{-/-}$→$Ldlr^{-/-}$] mice (Figure 3E, middle, 3F; $P = .006$), and IFN-γ–positive cells, probably lymphocytes, were detected at more significant numbers in [WT→$Ldlr^{-/-}$] chimeras than in [$CD1d^{-/-}$→$Ldlr^{-/-}$] chimeras (Figure 3E, lower). There were no overt differences in the staining patterns of α-smooth muscle actin and IL-10 between these 2 groups (data not shown). Mice reconstituted with syngeneic BMT ([$Ldlr^{-/-}$→$Ldlr^{-/-}$]) showed the same atherosclerotic lesions as those in [WT→$Ldlr^{-/-}$] mice (data not shown).

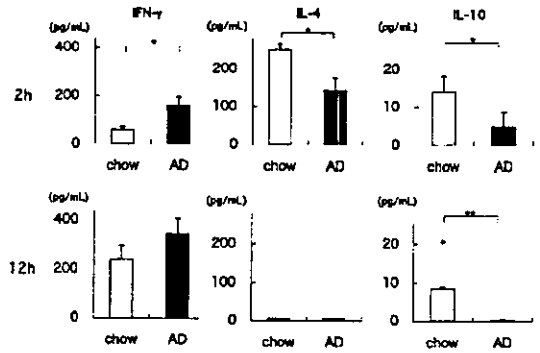

Figure 2. Production of cytokines by splenocytes from AD- or chow-fed WT mice treated with α-GalCer. Splenocytes were obtained from either AD- or chow-fed WT mice 2 or 12 hours after intravenous injection with 0.1 μg/g BW α-GalCer. Cells were cultured for 1.5 hours without additional stimulation. Culture supernatants were harvested, and IFN-γ, IL-4, and IL-10 levels were quantitated. Values are mean ± SE. Statistical analyses were performed using the Mann-Whitney *U* test. $^*P < .05$; $^{**}P < .01$.

Effects of NKT cell activation on the development of early atherosclerotic lesions in $apoE^{-/-}$ mice

To examine influences of NKT cell activation on the development of atherosclerosis, we administered α-GalCer or OCH to $apoE^{-/-}$ mice. $ApoE^{-/-}$ mice spontaneously develop severe atherosclerosis early in life.[8,9,35] It has been reported that α-GalCer and OCH activate NKT cells with differential patterns of cytokine production.[33]

In an early-phase study, $apoE^{-/-}$ mice were intraperitoneally injected 3 times with either 0.1 μg/g BW α-GalCer, 0.3 μg/g BW OCH or the respective vehicle at 8, 10, and 12 weeks of age. At 13 weeks of age, the mice were killed and examined for atherosclerotic lesions. No significant differences in physiologic status or serum lipid profiles were observed between experimental and control groups (α-GalCer or OCH vs their vehicle; data not shown). α-GalCer administration increased atherosclerotic lesion areas of $apoE^{-/-}$ mice compared with the vehicle control group (34 705 ± 5908 μm^2 vs 20 895 ± 2155 μm^2; $P = .039$) (Figure 4A-B). Major components of the atherosclerotic lesions in α-GalCer–treated mice included MOMA-2^+ macrophages (Figure 4C). OCH administration also increased atherosclerotic lesion areas compared with control (28 519 ± 2822 μm^2 vs 19 863 ± 1813 μm^2; $P = .048$) (Figure 4D). Lesion areas in the OCH-treated group, however, were relatively smaller than those in the α-GalCer–treated group. To determine a potential mechanism for the differences observed between the α-GalCer– and OCH-treated mice, we evaluated the sequential patterns of IFN-γ and IL-4 production in the serum after glycolipid injection. Both glycolipids induced robust cytokine production; however, though IL-4 production was similar, α-GalCer induced more IFN-γ than OCH, which is consistent with earlier findings (Figure 4E).[33]

Effects of long-term administration of α-GalCer on advanced atherosclerotic lesions in $apoE^{-/-}$ mice

In a late-phase study, we analyzed lesions in 19-week-old $apoE^{-/-}$ mice that had received 11 intraperitoneal injections of either α-GalCer or its vehicle. Again, no significant differences were observed in the physiologic status and serum lipid profiles between α-GalCer– and vehicle-treated mice (data not shown). Mean areas of lesions in the aortic sinus were slightly larger in the α-GalCer group than in the control group (197 448 ± 18 259 μm^2 vs 160 703 ± 16 320 μm^2) (Figure 5A). In

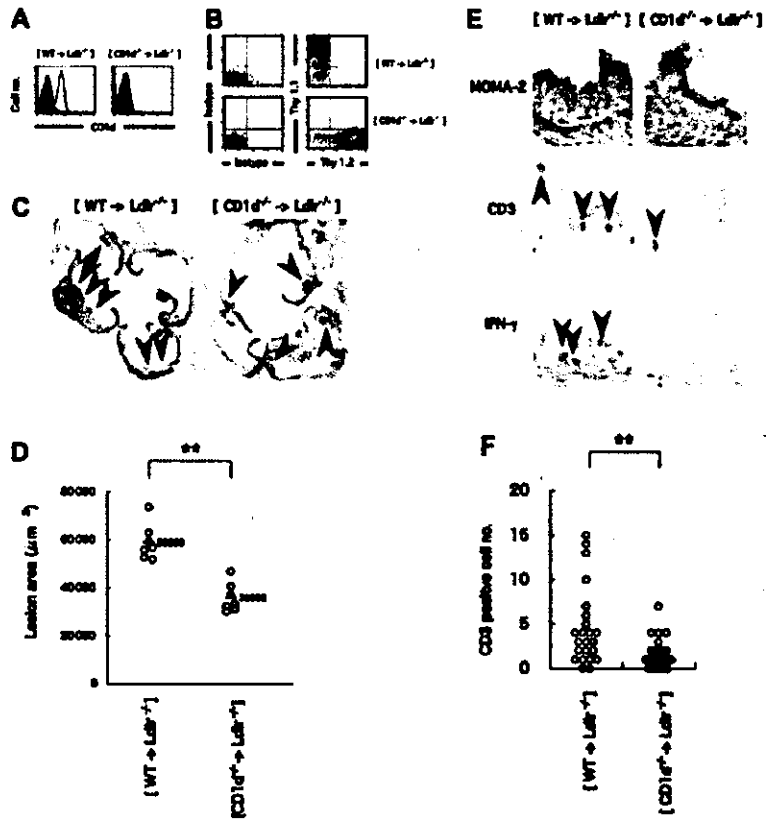

Figure 3. Atherosclerotic lesions in Ldlr$^{-/-}$ mice reconstituted with BM cells from CD1d$^{-/-}$ or WT mice. (A) Representative CD1d expression pattern on thymocytes from [WT→Ldlr$^{-/-}$] and [CD1d$^{-/-}$→Ldlr$^{-/-}$] mice. Red lines and filled histograms indicate CD1d staining and isotype control, respectively. (B) Thy1.1 and Thy1.2 expression on thymocytes from [WT→Ldlr$^{-/-}$] and [CD1d$^{-/-}$→Ldlr$^{-/-}$] chimeras. Representative results of Thy1.1 and Thy1.2 stainings are shown in the right panels with their respective isotype controls (left panels). (C) Representative histologic sections of [WT→Ldlr$^{-/-}$] and [CD1d$^{-/-}$→Ldlr$^{-/-}$] mice stained with oil red O (original magnification, × 40). Arrowheads represent oil red O–positive lesions. (D) Lesion area in [WT→Ldlr$^{-/-}$] and [CD1d$^{-/-}$→Ldlr$^{-/-}$] mice. Each symbol represents the lesion area of an individual mouse. Horizontal bars and numbers represent the mean of all mice within each group. $^{**}P < .01$ (E) Representative immunohistochemical section of [WT→Ldlr$^{-/-}$] and [CD1d$^{-/-}$→Ldlr$^{-/-}$] mice. Sections were stained with anti–MOMA-2, anti-CD3, and anti–IFN-γ mAb (original magnification, × 200). Arrowheads represent respective mAb-positive cells. (F) Numbers of CD3$^+$ cells per cross-section of lesion area. $^{**}P < .01$.

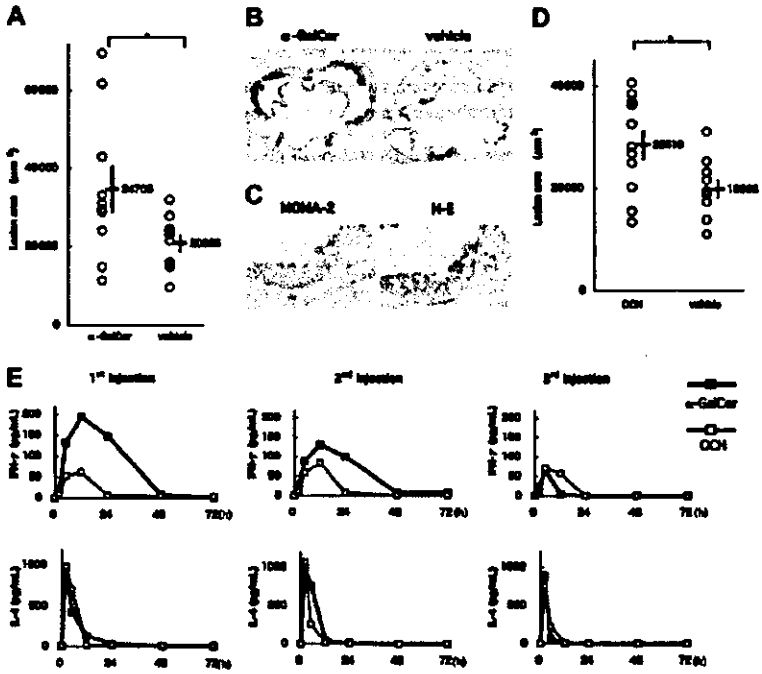

Figure 4. Effects of α-GalCer and OCH on the early phase of atherosclerosis. (A) ApoE$^{-/-}$ mice were intraperitoneally injected 3 times with α-GalCer or the vehicle alone, as described in "Materials and methods." Five weeks later, mice were examined for the development of atherosclerosis. Each symbol represents the lesion area of an individual mouse. Horizontal bars and numbers represent the mean of all mice within each group, and vertical bars represent SEM. (B) Representative histologic sections of the α-GalCer group and its control group stained with oil red O (original magnification, × 40). (C) Representative immunohistochemical section of the α-GalCer group stained with MOMA-2 and a serial section stained with hematoxylin and eosin (original magnification, × 200). (D) ApoE$^{-/-}$ mice were injected with OCH or vehicle. Mean lesion areas (OCH vs vehicle) are indicated as in Figure 4A. (E) Serum concentration of cytokines after administration of α-GalCer or OCH. Mean concentrations (n = 3) of IFN-γ (top) and IL-4 (bottom) in α-GalCer (■) and OCH (□) groups are shown after the first injection (left), the second injection (middle) and the third injection (right). Statistical analyses were performed using the Mann-Whitney *U* test. $^{*}P < .05$.

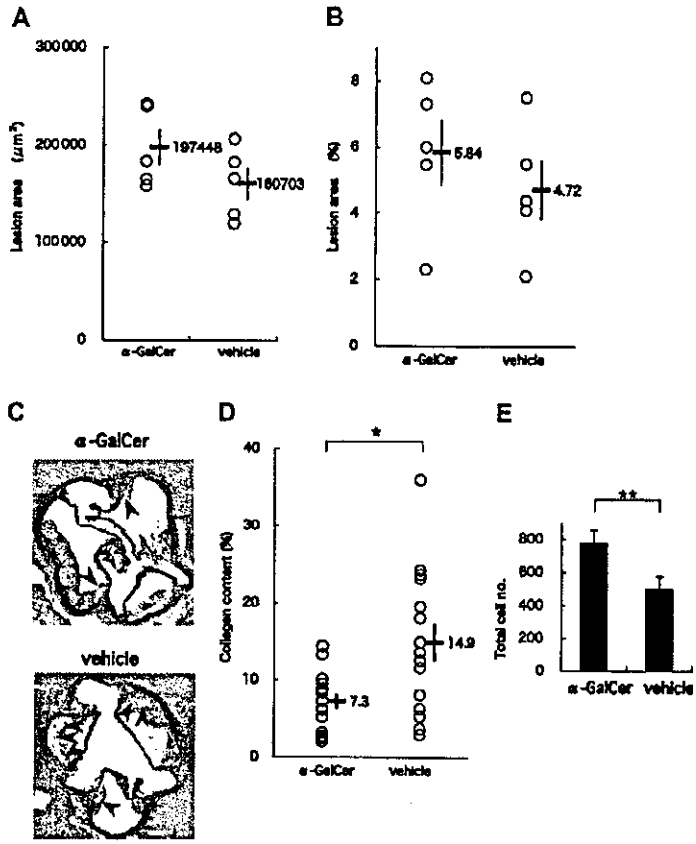

Figure 5. Effect of intensive α-GalCer administration on the late phase of atherosclerosis. ApoE$^{-/-}$ mice were injected weekly with α-GalCer or vehicle for a period of 11 weeks and examined for atherosclerosis at 19 weeks of age. (A) Mean lesion areas of each group are indicated as in Figure 4A. (B) Proportions of the oil red O–positive area to the whole lumen of the entire aorta were assessed by the en face method. (C) Representative histology of aortic sections from the α-GalCer group (top) or the control group (bottom) (Elastica-Masson staining). The collagen content is stained as blue in the lesion. Note that the blue region (arrowheads) in the α-GalCer–treated mouse is smaller than that in the control mouse. Original magnification, × 40. (D) Morphometric analysis of collagen contents of the atherosclerotic lesion. Mean lesion areas staining blue were quantitated with 3 aortic cross-sections per animal from a total of 10 animals. Statistical analyses were performed with the Mann-Whitney *U* test. $^{*}P < .05$. (E) Total cell numbers per cross-section of lesion area. Values are mean ± SE. $^{**}P < .01$.

addition, assessing lesion areas by the en face method showed slightly enlarged lesion areas in the α-GalCer group (5.8% ± 1.0%) compared with the control group (4.7% ± 0.9%) (Figure 5B). These results suggest that activating NKT cells exerts only slight influences on the development of advanced atherosclerotic lesions in apoE$^{-/-}$ mice. These findings are consistent with a previous report suggesting that lymphocytes are mostly involved in the early phase of atherogenesis.[6]

Figure 5C shows representative histologic analyses of the atherosclerotic lesions of α-GalCer– and vehicle-treated animals. Of note, the collagen content stained with Elastica-Masson was smaller in the α-GalCer–treated group than in the control group. When mean collagen content was compared between these 2 groups, the collagen content in the α-GalCer–treated group was significantly smaller than in the control group (7.3% ± 1.1% and 14.9% ± 2.4%, respectively; $P = .040$) (Figure 5D). However, the total cell number within the lesion per slice was significantly larger in the α-GalCer–treated group than in the control group (Figure 5E; $P = .009$). These findings suggest that NKT cell activation in the late phase of atherosclerosis alters the quality of the lesion from one rich in collagen to one characterized by high cellularity.

Vα14Jα18 TCR-α mRNA expression in atherosclerotic lesions of apoE$^{-/-}$ and AD-fed WT mice

Next, we examined atherosclerotic lesions by nested RT-PCR for detection of the invariant Vα14Jα18 TCR-α rearrangement characteristic of classic NKT cells. We were able to amplify the Vα14Jα18 rearrangement in the atherosclerotic tissues of apoE$^{-/-}$ mice and of WT mice on the AD (Figure 6), but we were unable to detect this rearrangement in the aortae of WT mice on the chow diet. Although we were unable to quantify numbers of NKT cells in the lesion, our results clearly demonstrated that the presence of Vα14Jα18-positive cells was restricted to the atherosclerotic lesions.

CD1d expression and IFN-γ production by WT peritoneal macrophages treated with LDL or OxLDL

Classic NKT cells recognize glycolipid antigens in the context of CD1d.[19,21,24-26,32,33] To investigate the mechanism by which NKT cells are activated and promote atherogenesis, peritoneal exudate

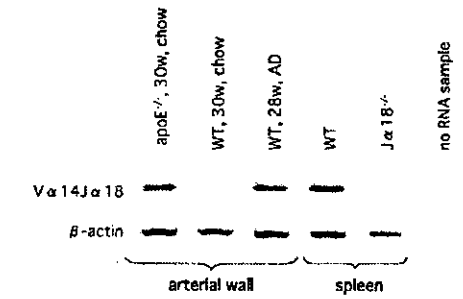

Figure 6. Vα14Jα18 mRNA in the atherosclerotic lesions. Expression of Vα14Jα18 mRNA in the atherosclerotic lesion was examined using RT-PCR. A sample from WT spleen was used as a positive control, and a sample from Jα18$^{-/-}$ spleen was used as a negative control. Note that Vα14Jα18 expression is detected only in the atherosclerotic tissues of apoE$^{-/-}$ mice (on the chow diet) and in WT mice on the AD. Representative result from 3 separate experiments is shown.

macrophages were harvested from WT mice, treated with LDL, OxLDL, or medium alone for 24 or 48 hours, and examined for expression of several surface molecules. The expression of CD1d on WT macrophages was enhanced by incubation with OxLDL for 24 hours, but not with LDL or medium alone (Figure 7A, top). No increase in the expression of MHC class I ($H\text{-}2K^b$) molecules was induced on macrophages by OxLDL (Figure 7A, bottom). In addition, OxLDL specifically enhanced CD1d expression in a dose-dependent manner (Figure 7B). No enhancement of $H\text{-}2K^b$, $I\text{-}A^b$ or CD40 expression was seen by treatment with LDL or OxLDL. When cultured for a longer time (48 hours) with OxLDL, CD1d expression was further augmented (Figure 7B). Of note, at a high dose (50 μg/mL) and after a long incubation period (48 hours), LDL enhanced CD1d levels on macrophages (Figure 7B).

We then examined whether the enhanced expression of CD1d on OxLDL-treated macrophages related to their capacity to stimulate NKT cells. We mixed HMNCs isolated from WT mice (containing 15%-30% NKT cells) with irradiated peritoneal macrophages from WT or $CD1d^{-/-}$ mice treated with LDL or OxLDL for 48 hours. After culture for 24 hours, IFN-γ and IL-4 levels in the supernatants were quantitated. NKT cells produced significantly higher amounts of IFN-γ in the cultures with OxLDL (50 μg/mL)–treated peritoneal exudate cells from WT mice compared with control cultures (Figure 7C). $CD1d^{-/-}$ macrophages treated in the same manner induced no enhancement of IFN-γ production. No IL-4 was detected in the supernatant in our culture conditions (data not shown).

Discussion

In this study we demonstrate, using 3 atherosclerosis models ($apoE^{+/+}$ mice fed with AD, $Ldlr^{-/-}$ chimeras fed with AD, and $apoE^{-/-}$ mice fed with normal chow), that NKT cells play a significant role in the development of atherosclerosis. In addition, we show that NKT cell activation modulates the disease process. Atherosclerotic lesion areas in AD-fed $CD1d^{-/-}$ mice were significantly smaller than those in AD-fed WT mice (Figure 1B). Because the development of invariant NKT cells is markedly hampered in $CD1d^{-/-}$ mice,[30] our findings suggest that NKT cell deficiency is related to the amelioration of atherosclerosis. It has been reported that AD induces inflammatory cytokines in the liver because of its high concentration of cholesterol and cholic acid[42] and that it may alter physiologic conditions. In the present study, WT and $CD1d^{-/-}$ mice were subjected to AD feeding in an identical manner. These 2 groups of mice showed comparable degrees of liver steatosis and similar levels of serum alanine aminotransferase and total bilirubin. Thus, we conclude that the significant differences in the atherosclerotic lesions between WT and $CD1d^{-/-}$ mice are directly related to the presence and absence, respectively, of the intact CD1d-restricted T-cell population.

The prevalence of NKT cells (mainly the CD1d/α-GalCer tetramer$^+$ fraction) among HMNCs of WT mice substantially decreased through the AD. A slight reduction of NKT cells was also observed in splenocytes of the AD-fed WT mice (Figure 1C). One characteristic of NKT cells is the prominent production of cytokines, IFN-γ, and IL-4 shortly after stimulation of these cells through the TCR.[22,41] We found that, despite their decreased NKT cell numbers, on stimulation with α-GalCer, spleen cells from AD-fed WT mice produced levels of IFN-γ, IL-4, and IL-10 comparable to those from chow-fed WT mice. Of note, the cytokine production pattern of spleen cell cultures of AD-fed WT mice shifted toward a T_H1 profile, especially 2 hours after α-GalCer stimulation (Figure 2). This pattern of cytokine production would be expected to promote atherosclerosis.[10-14] However, the mechanism underlying this altered cytokine production pattern, with the concomitant decrease of NKT cells, remains elusive. One possibility is that the decrease of NKT cells in AD-fed WT mice is caused by a depletion of this population by activation-induced cell death (AICD). This may be mediated by the CD1d-restricted presentation of lipid antigens such as OxLDL, which accumulate during hyperlipidemia. An alternative explanation would be that chronic stimulation of the NKT cell population results in the continuous down-modulation of NK1.1 and TCR marker expression, resulting in the apparent loss of these cells.[43] Furthermore, the diminished population of NKT cells could be attributed to the migration of

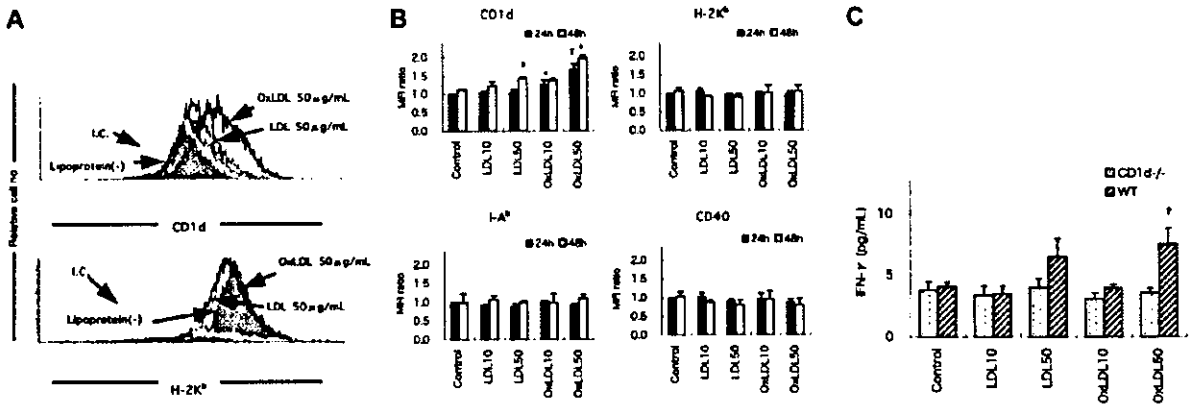

Figure 7. CD1d expression and IFN-γ production by WT peritoneal macrophages treated with LDL or OxLDL. WT peritoneal macrophages were treated with LDL or OxLDL or without additional lipoproteins (control) for 24 hours. (A) Representative histograms of CD1d or $H\text{-}2K^b$ expression on the macrophages. I.C. indicates each isotype control for either anti-CD1d or anti-$H\text{-}2K^b$ mAb. Cells with PI^{low} and Mac-1^{high} phenotypes were gated for analysis. (B) Mean fluorescence intensity (MFI) for CD1d, $H\text{-}2K^b$, $I\text{-}A^b$, or CD40 staining on WT peritoneal macrophages treated with LDL or OxLDL (10 or 50 μg/mL). Each column represents a ratio of MFI of a respective surface molecule to controls at either 24 hours (closed columns) or 48 hours (open columns). Values are mean ± SE of 3 independent experiments. *$P < .05$ vs control (24 hours). ‡$P < .01$ vs control, LDL10 or LDL50 (24 hours). §$P < .05$ vs control (48 hours). †$P < .01$ vs control, LDL10, LDL50, or OxLDL10 (48 hours). (C) Production of IFN-γ in the supernatant of the mixed culture of HMNCs with $CD1d^{-/-}$ or WT macrophages. HMNCs were cultured for 24 hours with peritoneal macrophages treated with LDL or OxLDL from $CD1d^{-/-}$ or WT mice. Then IFN-γ levels in the supernatant of the mixed culture were analyzed using ELISA. Values are mean ± SE of 3 independent experiments. †$P < .05$ vs control, LDL10, or OxLDL10 (WT). $P < .01$ vs OxLDL50 ($CD1d^{-/-}$).

these cells from liver or spleen to other peripheral tissues, such as the atherosclerotic lesion. In this context, we were able to detect mRNA corresponding to the invariant Vα14Jα18 TCR, which is characteristic of NKT cells and prerequisite for α-GalCer stimulation, within atherosclerotic lesions of AD-fed but not chow-fed WT mice by nested RT-PCR (Figure 6). The mechanisms that lead to NKT cell loss during AD feeding will be further addressed in future studies.

To examine the role of NKT cells in a more advanced atherosclerosis model, we reconstituted lethally irradiated $Ldlr^{-/-}$ mice with BM cells from $CD1d^{-/-}$ or WT mice. It has been reported that lack of LDL receptors aggravates the development of atherosclerosis in AD-fed mice. Indeed, using [WT→$Ldlr^{-/-}$] chimeras, Boisvert et al[44] reported that AD-fed chimeras showed severe atherosclerotic lesions where donor-derived leukocytes were present. In the present study, we observed that significantly large atherosclerotic lesions developed in [WT→$Ldlr^{-/-}$] chimeras compared with [$CD1d^{-/-}$→$Ldlr^{-/-}$] chimeras (Figure 3). These findings demonstrate that NKT cell deficiency indeed ameliorates atherosclerosis in AD-fed animals. Immunohistochemistry studies in this BMT model demonstrated that the number of $CD3^+$ cells within the lesion was significantly larger in [WT→$Ldlr^{-/-}$] than that in [$CD1d^{-/-}$→$Ldlr^{-/-}$] mice, suggesting that these $CD3^+$ cells contain NKT cells. Furthermore, we demonstrated NKT cell (Vα14Jα18) messages in lesions of other animal models by RT-PCR (Figure 6). However, immunohistochemical identification of NKT cells in the lesion has thus far been unsuccessful and will be pursued in future studies.

Complementary to the above results, we showed that activation of NKT cells by α-GalCer or OCH in $apoE^{-/-}$ mice, before significant lesions had been formed (early-phase study), resulted in increased areas of atherosclerotic lesions (Figure 4). We did not expect the results with OCH because it was reported that OCH favors a T_H2 shift of NKT cells.[33] It has been suggested that a T_H2 bias suppresses atherogenesis.[10,11] Consistent with previous reports,[33] we found that a single injection of α-GalCer induced prominent production of IFN-γ and IL-4, whereas OCH induced little IFN-γ but similar levels of IL-4 (Figure 4E). However, after multiple administrations, IFN-γ induction in response to α-GalCer became reduced to levels similar to those for OCH. In contrast, repeated injection of these glycoplipids did not alter IL-4 induction. Although a number of studies support the idea that the T_H1 cytokine IFN-γ is proatherogenic, the precise role of the T_H2 cytokine IL-4 in atherogenesis remains elusive.[45] Our finding that both α-GalCer and OCH exacerbate atherosclerosis during the early stage of the disease process, but to a different degree (Figure 4A, D), may be attributed to differences in the amounts and kinetics of IFN-γ and IL-4 production.

We found that peritoneal exudate macrophages expressed augmented levels of CD1d after culture with OxLDL (either 10 μg/mL or 50 μg/mL) or LDL (50 μg/mL) (Figure 7A-B). Although intact LDL is not captured by macrophages, it is plausible that LDL is degraded by peroxidases released from macrophages during the incubation period and is involved in the enhancement of CD1d expression. Furthermore, these macrophages with high CD1d expression stimulated NKT cells to produce low but significant levels of IFN-γ in vitro (Figure 7C). Thus, the enhancement of CD1d expression on OxLDL-pulsed macrophages appeared to result in their augmented capacity to induce IFN-γ production by HMNCs. This finding may be of importance because physiologically degraded lipids are abundantly present in the atherosclerotic lesions and may provide a source of physiologic ligands for NKT cells.

In the late-phase study to evaluate the effects of α-GalCer on atherosclerosis in $apoE^{-/-}$ mice, α-GalCer administration failed to enlarge lesions but instead decreased collagen content (Figure 5C-D) and increased total cell numbers (Figure 5E) within the atherosclerotic lesions. It has been reported that IFN-γ decreases collagen synthesis[13] and plays a role in plaque stability. Accordingly, it is possible that IFN-γ, which is produced on α-GalCer stimulation, decreases collagen synthesis. Thus, NKT cell activation at the late phase may alter the lesion structure from a stable to an unstable state. Ostos et al[29] demonstrated that LPS-treated $apoE^{-/-}$ mice have larger atherosclerotic lesions than PBS-treated control $apoE^{-/-}$ mice. In atherosclerotic lesions of these LPS-treated mice, increased numbers of IL-4–producing $NK1.1^+$ cells were detected by immunohistochemistry. In our present study, the invariant Vα14Jα18 TCR was detected in aortic specimens with atherosclerotic lesions of either AD-fed WT or $apoE^{-/-}$ mice (Figure 6). These findings again favor the idea that NKT cells play a proatherogenic role in situ. However, it is also possible that NKT cells are activated in other tissues, such as the liver or spleen, and systemically affect the atherogenic process. Thus, the precise location where NKT cells are activated and demonstrate their effector functions during progression of atherosclerosis remains to be elucidated. Although T_H1 and T_H2 cytokines are probably important, other factors, such as chemokines and the capacity of NKT cells to exhibit cytotoxicity, should be considered in further investigations.[23,34] In summary, we have demonstrated that NKT cells accelerate atherogenesis in mouse models for this disease. In addition, we show that NKT cell activation in the early phase of the disease process exacerbates atherogenesis and that NKT cell activation in the late phase of the disease promotes plaque instability. Because NKT cells and CD1d molecules are highly conserved among different species,[46] our present results may be applicable to elucidation of the pathophysiology of atherosclerosis in humans, and they offer a novel approach for controlling the atherogenic process by intervening with certain NKT cell functions.

Acknowledgments

We thank the staffs at Kirin Brewery Company and Takeda Chemical Industries for providing α-GalCer and recombinant human IL-2, respectively. We also thank Keiko Kato and Mizuho Kasai for technical assistance.

References

1. Ross R. Atherosclerosis—an inflammatory disease. N Engl J Med. 1999;340:115-126.
2. Binder CJ, Horkko S, Dewan A, et al. Innate and acquired immunity in atherogenesis. Nat Med. 2002;8:1218-1226.
3. Hansson GK, Libby P, Shoebeck U, Yan ZQ. Innate and adaptive immunity in the pathogenesis of atherosclerosis. Circ Res. 2002;91:281-291.
4. Jonasson L, Holm J, Skalli O, Bondjers G, Hansson GK. Regional accumulations of T cells, macrophages, and smooth muscle cells in the human atherosclerotic plaque. Arteriosclerosis. 1986;6:131-138.
5. Roselaar SE, Kakkanathu PX, Daugherty A. Lymphocyte populations in atherosclerotic lesions of $apoE^{-/-}$ and LDL $receptor^{-/-}$ mice: decreasing density with disease progression. Arterioscler Thromb Vasc Biol. 1996;16:1013-1018.
6. Song L, Leung C, Schindler C. Lymphocytes are important in early atherosclerosis. J Clin Invest. 2001;108:251-259.
7. Dansky HM, Charlton SA, Harper MM, Smith JD. T and B lymphocytes play a minor role in atherosclerotic plaque formation in the apolipoprotein

E-deficient mouse. Proc Natl Acad Sci U S A. 1997;94:4642-4646.

8. Reardon CA, Blachowicz L, White T, et al. Effect of immune deficiency on lipoproteins and atherosclerosis in male apolipoprotein E–deficient mice. Arterioscler Thromb Vasc Biol. 2001;21:1011-1016.
9. Zhou X, Nicoletti A, Elhage R, Hansson GK. Transfer of CD4+ T cells aggravates atherosclerosis in immunodeficient apolipoprotein E knockout mice. Circulation. 2000;102:2919-2922.
10. Huber SA, Sakkinen P, David C, Newell MK, Tracy RP. T-helper-cell phenotype regulates atherosclerosis in mice under conditions of mild hypercholesterolemia. Circulation. 2001;103:2610-2616.
11. Laurat E, Poirier B, Tupin E, et al. In vivo downregulation of T helper cell 1 immune responses reduces atherogenesis in apolipoprotein E–knockout mice. Circulation. 2001;104:197-202.
12. Gupta S, Pablo AM, Jiang X, Wang N, Tall AR, Schindler C. IFN-γ potentiates atherosclerosis in apoE knock-out mice. J Clin Invest. 1997;99:2752-2761.
13. Whitman SC, Ravisankar P, Elam H, Daugherty A. Exogenous interferon-γ enhances atherosclerosis in apolipoprotein $E^{-/-}$ mice. Am J Pathol. 2000;157:1819-1824.
14. Tellides G, Tereb DA, Kirkiles-Smith NC, et al. Interferon-γ elicits arteriosclerosis in the absence of leukocytes. Nature. 2000;403:207-211.
15. Lee TS, Yen HC, Pan CC, Chau LY. The role of interleukin-12 in the development of atherosclerosis in apoE-deficient mice. Arterioscler Thromb Vasc Biol. 1999;19:734-742.
16. Pinderski LJ, Fischbein MP, Subbanagounder G, et al. Overexpression of interleukin-10 by activated T lymphocytes inhibits atherosclerosis in LDL receptor-deficient mice by altering lymphocyte and macrophage phenotypes. Circ Rec. 2001;89:930-934.
17. Caligiuri G, Nicoletti A, Poirier B, Hansson GK. Protective immunity carried by B cells of hypercholesterolemic mice. J Clin Invest. 2002;109:745-753.
18. Major AS, Fazio S, Linton MF. B-lymphocyte deficiency increases atherosclerosis in LDL receptor-null mice. Arterioscler Thromb Vasc Biol. 2002;22:1892-1898.
19. Godfrey DI, Hammond KJ, Poulton LD, Smyth MJ, Baxter AG. NKT cells: fact, functions and fallacies. Immunol Today. 2000;21:573-583.
20. Wilson MT, Singh AK, Van Kaer L. Immunotherapy with ligands of natural killer T cells. Trends Mol Med. 2002;8:225-231.
21. Arase H, Arase N, Ogasawara K, Good RA, Onoé K. An NK1.1+ $CD4^+8^-$ single-positive thymocyte subpopulation that expresses a highly skewed T-cell antigen receptor Vβ family. Proc Natl Acad Sci U S A. 1992;89:6506-6510.
22. Arase H, Arase N, Nakagawa K, Good RA, Onoé K. NK1.1+ $CD4^+8^-$ thymocytes with specific lymphokine secretion. Eur J Immunol. 1993;23:307-310.
23. Arase H, Arase N, Kobayashi Y, et al. Cytotoxicity of fresh NK1.1+ T cell receptor $\alpha\beta^+$ thymocytes against a $CD4^+8^+$ thymocyte population associated with intact Fas expression on the target. J Exp Med. 1994;180:423-432.
24. Singh N, Hong S, Scherer DC, et al. Activation of NK T cells by CD1d and α-galactosylceramide directs conventional T cells to the acquisition of a Th2 phenotype. J Immunol. 1999;163:2373-2377.
25. Burdin N, Brossay L, Kronenberg M. Immunization with α-galactosylceramide polarizes CD1-reactive NK T cells towards Th2 cytokine synthesis. Eur J Immunol. 1999;29:2014-2025.
26. Cui J, Watanabe N, Kawano T, et al. Inhibition of T helper cell type 2 cell differentiation and immunoglobulin E response by ligand-activated Vα14 natural killer T cells. J Exp Med. 1999;190:783-792.
27. Melian A, Geng YJ, Sukhova GK, Libby P, Porcelli SA. CD1 expression in human atherosclerosis: a potential mechanism for T cell activation by foam cells. Am J Pathol. 1999;155:775-786.
28. Piedrahita JA, Zhang SH, Hagaman JR, Oliver PM, Maeda N. Generation of mice carrying a mutant apolipoprotein E gene inactivated by gene targeting in embryonic stem cells. Proc Natl Acad Sci U S A. 1992;89:4471-4475.
29. Ostos MA, Recalde D, Zakin MM, Scott-Algara D. Implication of natural killer T cells in atherosclerosis development during a LPS-induced chronic inflammation. FEBS Lett. 2002;519:23-29.
30. Mendiratta SK, Martin WD, Hong S, Boesteanu A, Joyce S, Van Kaer L. CD1d1 mutant mice are deficient in natural T cells that promptly produce IL-4. Immunity. 1997;6:469-477.
31. Ishibashi S, Brown MS, Goldstein JL, et al. Hypercholesterolemia in low density lipoprotein receptor knockout mice and its reversal by adenovirus-mediated gene delivery. J Clin Invest. 1993;92:883-893.
32. Kawano T, Cui J, Koezuka Y, et al. CD1d-restricted and TCR-mediated activation of Vα14 NKT cells by glycosylceramides. Science. 1997;278:1626-1629.
33. Miyamoto K, Miyake S, Yamamura T. A synthetic glycolipid prevents autoimmune encephalomyelitis by inducing T_H2 bias of natural killer T cells. Nature. 2001;413:531-534.
34. Cui J, Shin T, Kawano T, et al. Requirement for Vα14 NKT cells in IL-12–mediated rejection of tumors. Science. 1997;278:1623-1626.
35. Ishimori N, Iwabuchi K, Fujii S, et al. Mixed allogenic chimerism with wild-type strains ameliorates atherosclerosis in apolipoprotein E-deficient mice. J Leukoc Biol. 2001;69:732-740.
36. Paigen B, Morrow A, Holmes PA, Mitchell D, Williams RA. Quantitative assessment of atherosclerotic lesions in mice. Atherosclerosis. 1987;68:231-240.
37. Ato M, Iwabuchi K, Shimada S, Mukaida N, Onoé K. Augmented expression of tumor necrosis factor-α induced by lipopolysaccharide in spleen of human monocyte chemoattractant protein-1 transgenic mouse enhances the lipopolysaccharide sensitivity of the marginal zone macrophages. Immunology. 2002;106:554-563.
38. Iwabuchi K, Iwabuchi C, Tone S, et al. Defective development of NK1.1+ T-cell antigen receptor α/β^+ cells in zeta-associated protein 70 null mice with an accumulation of NK1.1+ $CD3^-$ NK-like cells in the thymus. Blood. 2001;97:1765-1775.
39. Watanabe H, Ohtsuka K, Kimura M, et al. Details of an isolation method for hepatic mononuclear cells in mice. J Immunol Methods. 1992;146:145-154.
40. Stanic AK, De Silva AD, Park JJ, et al. Defective presentation of the CD1d1-restricted natural Vα14Jα18 NKT lymphocyte antigen caused by β-D-glucosylceramide synthase deficiency. Proc Natl Acad Sci U S A. 2003;100:1849-1854.
41. Yoshimoto T, Bendelac A, Hu-Li J, Paul WE. Defective IgE production by SJL mice is linked to the absence of $CD4^+$, NK1.1+ T cells that promptly produce interleukin 4. Proc Natl Acad Sci U S A. 1995;92:11931-11934.
42. Berliner JA, Navab M, Fogelman AM, et al. Atherosclerosis, basic mechanisms: oxidation, inflammation, and genetics. Circulation. 1995;91:2488-2496.
43. Wilson MT, Johansson C, Olivares-Villagomez D, et al. The response of natural killer T cells to glycolipid antigens is characterized by surface receptor down-modulation and expansion. Proc Natl Acad Sci U S A. 2003;100:10913-10918.
44. Boisvert WA, Spangenberg J, Curtiss LK. Role of leukocyte-specific LDL receptors on plasma lipoprotein cholesterol and atherosclerosis in mice. Arterioscler Thromb Vasc Biol. 1997;17:340-347.
45. King VL, Szilvassy SJ, Daugherty A. Interleukin-4 deficiency decreases atherosclerotic lesion formation in a site-specific manner in female LDL receptor$^{-/-}$ mice. Arterioscler Thromb Vasc Biol. 2002;22:456-461.
46. Brossay L, Chioda M, Burdin N, et al. CD1d-mediated recognition of an α-glycosylceramide by natural killer T cells is highly conserved through mammalian evolution. J Exp Med. 1998;188:1521-1528.